Observing changes of the Hargen dunes using annual LiDAR data

Floor Hoekstra

Delft University of Technology

TU Delft

Project duration: May, 2024 – July, 2024
Supervisors: R.C. Lindenbergh
D.C. Hulskemper
S.E. Vos

Abstract

In 2003, the Hondsbossche and Pettemer Zeewering, located from Camperduin to Petten, was classified to not be within safety margins of the Dutch Coast. In order to protect the Dutch Coast from sea level rise, the Hondsbossche dunes were created in 2015. This project included the building of an artificial lagoon for recreational purposes. This lagoon is protected from the sea by three sand dunes. Without these dunes, the lagoon will not remain to exist. The aim of this study is to detect changes of the shape and the height of the dunes protecting the lagoon at Camperduin from the sea using annual lidar data.

JARKUS data is obtained from airborne laser scanning for the Dutch coastal areas which is done yearly between January and March. Eight datasets of annual lidar data which include the dunes are used for this study. The datasets consists of point clouds for the years 2016 to 2023.

To obtain information about the changes occurring, several methods are used. The workflow recommended is the C2M method for 3D changes. These changes can be clustered by K-means clustering. 2D changes can be observed using cross sections, contour lines and the volume changes.

The seaward side of the dunes decreases in height due to marine erosion such as storms. Around 4.5 meter erosion on some locations has been found due to large storms in 2022. The lagoon side of the dunes increases in height by aeolian transport. The rate of dune growth is found to be 0.5 meters per year.

The middle dune experiences more erosion than deposition and the volume decreases. The erosion is caused by less vegetation and human impacts. If the trend from before the storm in 2022 continues, the dune will shrink and disappear if no additional maintenance is done. The other two dunes do not experience big volume losses and are classified as stable.

Contents

1

Introduction

In 2003, it was observed that multiple locations on the Dutch Coast were not within safety margins (Deltares, 2019). For this, the program ”Zwakke Schakels Kust” was made, which indicates eight weak links of the Dutch coasts, including the Hondsbossche and Pettemer Zeewering, located from Camperduin in the south to Petten in the north. From 2014 to 2015, this part of the coast was reinforced by a joint venture of Van Oord and Boskalis. In front of the existing dike, 35 million cubic meters of sand was used to create a natural barrier of sand along the 8 km coast of Camperduin to Petten. This project was part of the program Building with Nature (HKV, 2020), which protects the Netherlands from sea level rise for the next 50 years. The new dunes were called the Hondsbossche Dunes, seen in figure 1.1. By adding sand instead of increasing the height of the current dike, there were more possibilities for tourism and nature (Hoogheemraadschap Hollands Noorderkwartier et al., n.d.). In the middle part, more space is given to nature, while in the north and the south near the villages, the focus is more on tourism and recreational areas. This is also the reason of why an artificial lagoon is built near Camperduin, which is mainly used for water sports.

The lagoon cannot sustain on its own and requires regular maintenance to keep the access to the sea open and therefore sustain the water quality. The dunes on the west side of the lagoon shield the lagoon from the tides and waves. It creates a safe environment for watersports which would not be the case without these dunes.
The maintenance of the lagoon and dunes was done by van Oord & Boskalis until 2020. After this year, the local council Gemeente Bergen asked the inhabitants if they would like it if the lagoon stayed open. Most of the inhabitants did like the lagoon and therefore it was decided to stay open with funding of Gemeente Bergen. This was agreed to be for the next four years. In 2023, Hoogheemraadschap Hollands Noorderkwartier (HHNK) and Rijkswaterstaat proposed to only sustain the water safety aspect of the Hondsbossche Dunes, and not the recreational services. The reason for this was the presence of heavy currents in the sea which sweep away a lot of sand from the beach. Therefore, the maintenance was more expensive than initially expected. To postpone the decision of what to sustain, a foreshore nourishment will be done in

Figure 1.1: Location of the Hondsbossche Dunes and the study area (Bodde et al., 2019). Site location 52.72°N 4.63°E.

2025. This sand will spread gradually over the coast and makes sure the current beach does not wear out too fast (Gemeente Schagen, 2024). It will be the question if the lagoon still exists in the future.

To be able to see how the dunes are changing over time, remote sensing techniques can be used. Remote sensing is an efficient way to map the surface of the earth by the use of airplanes or satellites. An example of a remote sensing technique is LiDAR which stands for Light Detection and Ranging. A laser pulse is sent towards the surface from an airplane and by using the speed of light, the distance to the earth can be calculated. Together with the location of the plane, the measurements can be converted to a 3D point cloud which represents surface.
Lidar data is widely used in the Netherlands. Every few years, the entirety of the Netherlands is mapped and the Dutch Coast is mapped annually. Comparing the point clouds of each year can be used to quantify changes of the coast.

1.1. Research questions

The dunes on the west side of the lagoon were man made in 2015. It will be interesting to see how these artifical dunes change over time.
In this study, the behaviour of the dunes on the seaward side of the lagoon is studied using laser altimetry data. The research question for this is:

How can changes of the shape and the height of the dunes protecting the lagoon at Camperduin from the sea be detected using annual lidar data from 2016 to 2023?

To be able to answer this, a few sub-questions need to be answered first:

- How is lidar data obtained and how can it be used to quantify changes?
- What are good methods to detect changes in the dunes?
- Where do the greatest changes occur in the dunes?

1.2. Scope of research

To be able to do this research, airborne lidar data is used. The yearly lidar data from 2016 to 2023 is used (GeoTiles & Rijkswaterstaat, 2023), since the data of 2024 was not available yet at the moment of this study. The main focus lies on how changes in the dunes can be detected and it only discussed shortly what the reasons are of these changes.

1.3. Thesis outline

This thesis begins with chapter 2, which discusses the monitoring of the lagoon, processes on the beach and introduces the working of airborne lidar data. In chapter 3, the research area is described and information about the data set is given. This is followed with the methodology of detecting changes using lidar data in chapter 4. The results of these methods are found in chapter 5. Chapter 6 provides a discussion of the results. In chapter 7, a final conclusion is given and the research questions are answered. Also, recommendations are given for further research.

2

Monitoring of the lagoon

To be able to assess how changes can be monitored, it must be understood what regular change processes occur at the beach and in the dunes. In this chapter, some of the characteristics of the beach will be discussed like processes on the beach, natural and anthropogenic. Next, it will be discussed how lidar data is obtained, together with the accuracy and the limitations.

2.1. Characteristics of the beach

The Dutch coast line exists of sandy beaches. These sandy beach-dune systems can be subdivided in different components, depending on elevation, contact with the water and type of sedimentation and erosion. The main categories are the emerged beach and the submerged beach. The emerged beach consists of the back shore and the foreshore. The back shore is more land inward and on higher elevation. The dunes are an example of the back shore. This part is not affected by waves, unless there is a storm present. On the back shore, the most erosion is done by the wind (Longhitano, 2015). The foreshore is influenced by the sea and the boundaries are determined by the high and the low tide. These are the maximum and minimum water levels (excluding storms). Therefore the foreshore is also called the intertidal zone. This zone also includes the swash zone where the waves roll over the beach and moves materials up and down the beach (Longhitano, 2015). The submerged beach is constantly lying under the water line where it is subjected to water motions, such as waves and tides. The different zones of the beach can be seen in figure 2.1.
This study focuses on the dunes, which are a part of the back shore.

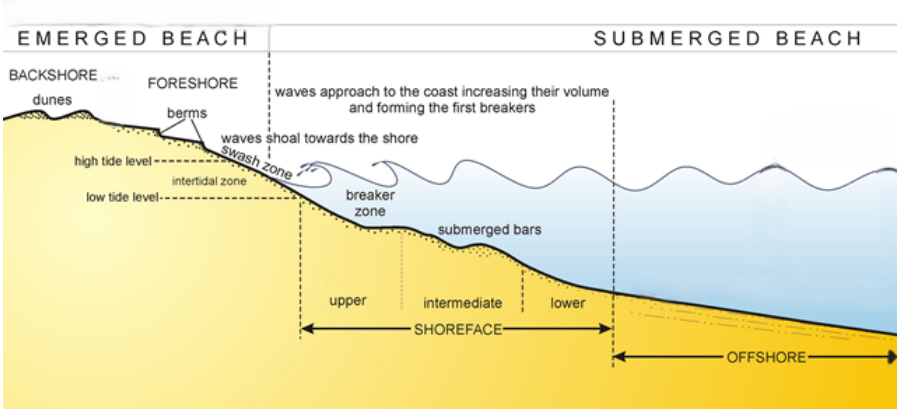

Figure 2.1: Cross-shore beach partitioning showing subaerial and subaqueous environments and sub-environments. Modified from Longhitano, 2015.

2.2. Processes at the beach

There are many processes on the beach. These can be subdivided in natural and anthropogenic processes. Both of these will be discussed in the following sub-sections.

2.2.1. Natural processes

The beach and the dunes are environments that are constantly changing. Various natural factors, such as wind, tides and storms are processes which influence the shape and the size of the beach and the dunes.

Aeolian

The aeolian processes mainly influence the dry sediments. These also include the loose sediments which are only exposed at low tide on the intertidal zone. These dry out and can be transported by the wind (Nichols, 2009). First, ripples can be formed which can continue to grow into new dunes. This study will focus on the movement of existing dunes. Not only new dunes can be accommodated by aeolian processes, it also influences existing structures. Dunes can migrate due to sand particles being picked up by the wind and deposited on the other side of the dune. How fast this happens, is dependent on the wind speed and other factors. The process is shown in figure 2.2.

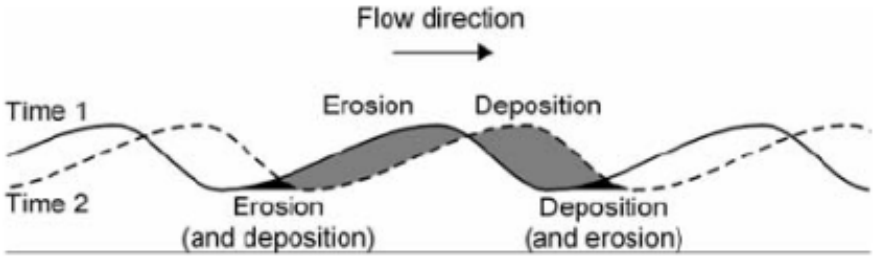

Figure 2.2: The process of dune forming (Ernstsen et al., 2007)

The dunes protecting the lagoon from the sea are human made. These are changed due to natural processes. On the east side of the lagoon, the dunes are naturally created.

The timescale of different processes on the beach are shown in figure 2.3. The smaller timescale processes (hours - days) mainly happen on the beach and not in the dunes. When looking at the years to decades scale, the change of beach position, large size beach cycles and major storm erosion is given. Large size beach cycles also include the movement of dunes. It is therefore expected from this study with annual data to see the movement of dunes and the impact of storm erosion.

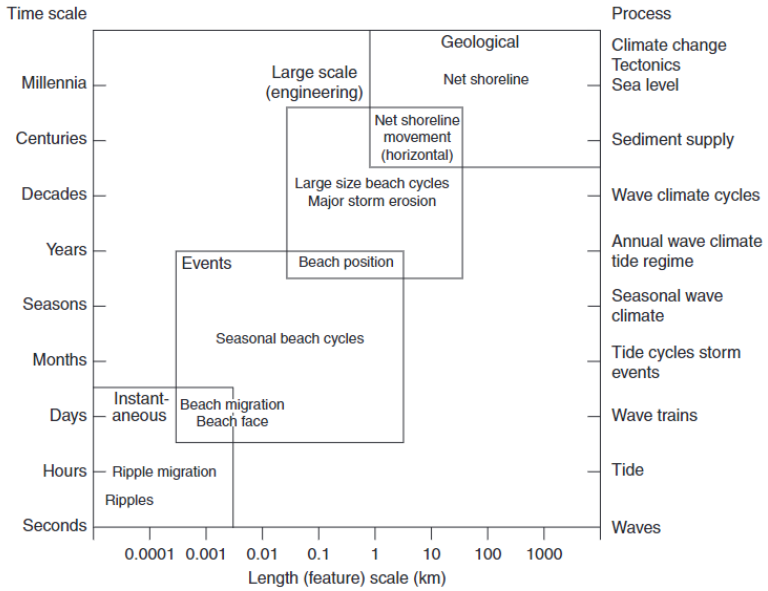

Figure 2.3: Relationship between the scale of coastal sedimentary features and their temporal variability (Short & Jackson, 2013).

Tides
The tides mainly influence the intertidal zone. For different times in the year, the place of the high and the low tide are different and therefore the location of where aeolian transport can take place differ (Smith, 1986). Intertidal bars can be formed on sandy and pebble beaches. These are formed by sediments which are moved underwater towards the beach. Once the water drops to low tide, the bars are above the water line and dry. These sediments can be transported by wind and feed the dunes. The intertidal bars are an important phenomenon since it is the transition between marine and aeolian sediment transport (Vos et al., 2020). The intertidal bars are not further discussed in this study, but it is important to keep in mind that dunes grow mainly due to sediment transport of intertidal bars.

Storms
Storms can affect land and marine environments. Due to the high energy, the sea floor is heavily reworked and this brings many sediments in suspension (Nichols, 2009). In combination with heavy winds and high water, the water can come to a higher place than it normally does and sweep away part of the dunes.

2.2.2. Anthropogenic processes
Next to natural activity, there is also anthropogenic activity on the beach. Anthropogenic activity is an activity that is human made. These kind of activities include the construction of buildings on the beach, such as (seasonal) beach restaurants and accommodations for tourists. There are also often bulldozers driving around to clean up unwanted piles of sand and to open up channels. Lastly, dunes are sometimes artificially created and sand nourishments are done.
Anthropogenic processes that influenced the data are discussed in chapter 6.

2.3. Lidar data
Lidar is the abbreviation of Light Detection and Ranging. This is a remote sensing technology which can create dense measurements of the surface of the earth and create a 3D visual representation (Vosselman & Maas, 2010). The measurements contain information about the x-, y- and z-direction of the location (Harikumar, 2020). For lidar, a laser pulse is transmitted from an optical sensor. This optical sensor is located on an aircraft if airborne laser scanning is used and transmits a near-infrared laser for topographic mapping. After the laser has hit the target, it is reflected and this reflection can be detected by receivers on the aircraft. Using the time of when the laser pulse left and returned and the speed of light, the distance to the target can be calculated (Harikumar, 2020). To be able to

convert the measurements to a 3D point cloud, the Global Positioning System (GPS) and the Inertial Measurement Unit (IMU) must be known. The IMU measures the velocity of the airplane and the orientation (Vosselman & Maas, 2010) and GPS gives the exact location. The principle of airborne laser scanning can be seen in figure 2.4.

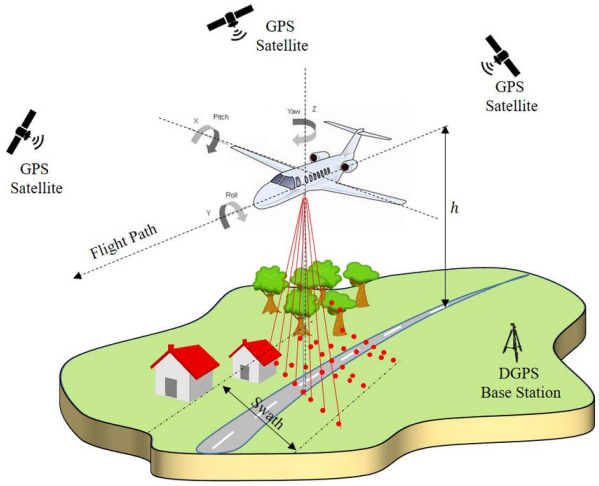

Figure 2.4: The principle of airborne laser scanning (Harikumar, 2020).

2.3.1. Quality

The coordinates of the lidar data are expressed in RD-coordinates, which stands for Rijksdriehoekstelsel which is the standard coordinate system used in the Netherlands. The height is given in NAP which stands for Normaal Amsterdams Peil.

Errors that might be present in the data are random errors and systematic errors. Random errors are always present. A systematic error is an error in the data due to inaccuracy of the measuring instruments. Examples of systematic errors in airborne laser scanning data are the range error, scan angle error, GPS and IMU errors (Wang et al., 2008).

2.3.2. Limitations

A big limitation of lidar data is that it does not return information about water surfaces, if near-infrared laser is used. This laser cannot penetrate through the water to measure the surface beneath. The water bodies absorb part of the laser radiation instead of reflecting it (Vosselman & Maas, 2010), which can provide information about the extent of the water body and only partially about the surface beneath the water.

3

Area description and data set

This chapter will elaborate more on the area of interest in this study and the characteristics of the data set used. Some important parameters of the data and events that happened will also be discussed.

3.1. Area description

As described in the introduction, the area to be studied are the three dunes protecting the lagoon from the sea, located near Camperduin and Hargen aan Zee. The design of this lagoon is visualised in figure 3.1a. The front dunes consists of three different dunes which are the subject of this study.

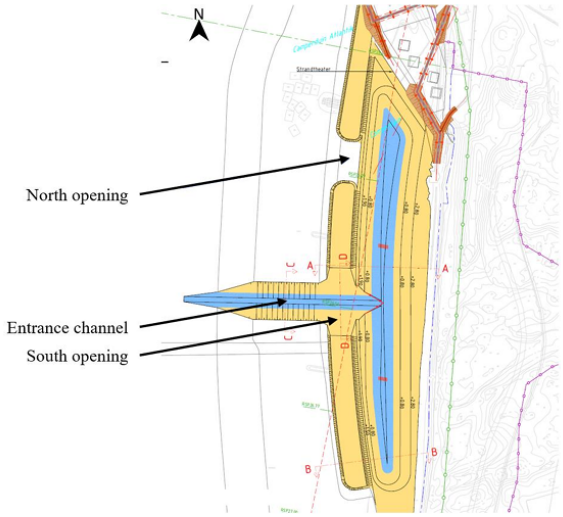

(a) Lagoon design. It is located parallel to the coast and sheltered by front dunes. These front dunes have two openings, a north opening and a south opening. The entrance channel is located in the south opening, connecting the lagoon with the sea (Jacobs, 2019)

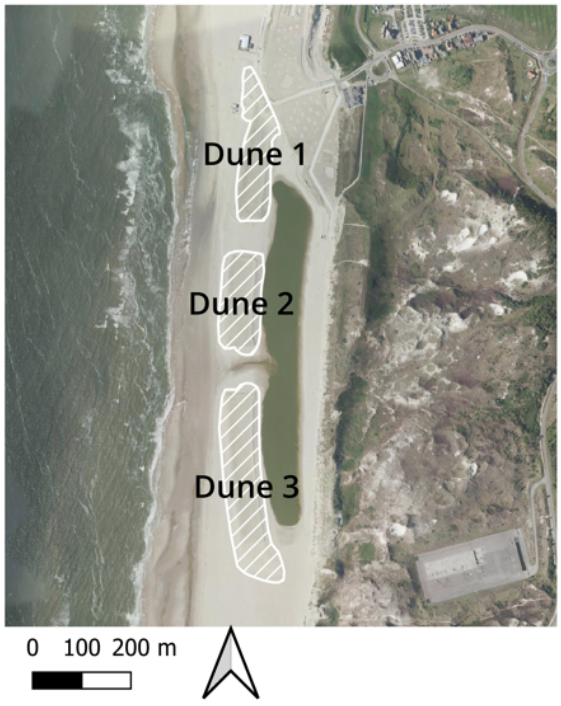

(b) The three dunes numbered. These numbers will be used in the rest of the report. The aerial photo of 2016 is used (GeoTiles & Rijkswaterstaat, 2023).

Figure 3.1: The dunes protecting the lagoon from the sea.

3.1.1. Maintenance of the lagoon

The maintenance of the lagoon includes dredging of the channel. This is mainly done just before the summer season. The dredging must also be done if the water quality is below the safety standards. By opening the channel, the water quality will increase. The water quality is monitored every two weeks in the summer season. The dates on which dredging occurred are shown in figure 3.2. This data was only available until 2019. For the years after, it is unknown at what dates dredging occurred, but assumed to also be before the summer season.

Date	Reason:
7-4-2016	Before summer season, to support recreation season
12&13-6-2017	Before summer season. Channel open whole winter, therefore dredging was later in year.
28&29-6-2017	Diminished water quality
9-4-2018	Before summer season, to support recreation season
10&11-7-2018	Unclear
30-7-2018	Diminished water quality
24-4-2019	Before summer season, to support recreation season
5-7-2019	Unclear

Figure 3.2: Channel dredging moments and reasons (Jacobs, 2019)

3.1.2. Climatic conditions of the area

The most common wind direction in the Netherlands is from the southwest (Janssen, 2021). Storms occur regularly, especially in the winter and early spring season. For very heavy weather event, the Dutch weather institute (KNMI) can give a code red warning. This was the case for February 16th to February 20th 2022 and January 18th 2018 (KNMI, n.d.). In 2022, three storms went over the Netherlands within those four days. One of those storms was in the top three of heaviest storms in the last 50 years.
The data of the years 2018 and 2022 may be influenced by these storms.

3.2. Data set

Multiple data sources are available for the research area. The main objective of this thesis is to quantify the changes using lidar data, for which JARKUS data is used. To get a general overview of the area and how it changes over the year, aerial photos are used. These are not taken at the same dates as the JARKUS data, but a few months later. Overall, all the data is taken between January and May, which is approximately the same season.

3.2.1. JARKUS data

In order to identify any changes to the front dunes, data from the JARKUS database is used. JARKUS is a yearly coast measurement of the Netherlands and determines the coast line. For this study, only the laser measurements are used on the dry parts and not the bathymetric measurements in the water. The JARKUS data is owned by Rijkswaterstaat and is freely available for the years 2016-2023 as point clouds. The data is retrieved from GeoTiles and Rijkswaterstaat, 2023. The measurements are made between January and April for each year (Actueel Hoogtebestand Nederland, 2019).

Table 3.1: File creation data and point density of the original file (GeoTiles & Rijkswaterstaat, 2023)

File creation date	Point density (returns per m^2)
16-02-2016	4.89
27-01-2017	4.49
13-02-2018	7.33
24-02-2019	6.70
14-03-2020	6.95
15-01-2021	8.38
28-02-2022	11.87
08-02-2023	5.34

The systematic error of the data may not be larger than 5 cm. The standard deviation of the height data is maximum 10 cm with clear sand and 30 cm with vegetation (Actueel Hoogtebestand Nederland, 2019; Vos et al., 2024). The point density needs to be at least 1 point per 2 m^2 for the Dutch coast. This is a minimum requirement and as seen in table 3.1, the actual point density is much higher. It is unknown if the point density also takes into account the areas where there are no measurements, such as the lagoon, or not. The point density is only known for the original file.

It is seen that the data of 2018 and 2022 are taken after the storms that went over the Netherlands (section 3.1.2). In 2022, there are only a few days between the storms and the data collection.
The data in 2018 was collected around a month after the storm. It could be that it still shows some signs of the storms, but it is expected to be less than in 2022.

3.2.2. Aerial photos

Other data that is available are aerial photos. These however are not taken at the same date as the lidar data. All the photos are taken on the 15th of May (GeoTiles & Rijkswaterstaat, 2023). This is later than the lidar data. It can be seen that in the years up to 2019, the channel has been opened before the picture was taken. After 2019, the channel was closed the majority of the time.
The aerial photos are mainly used to get a first impression of the area and to see how the shape of the dunes and the lagoon change over the years.

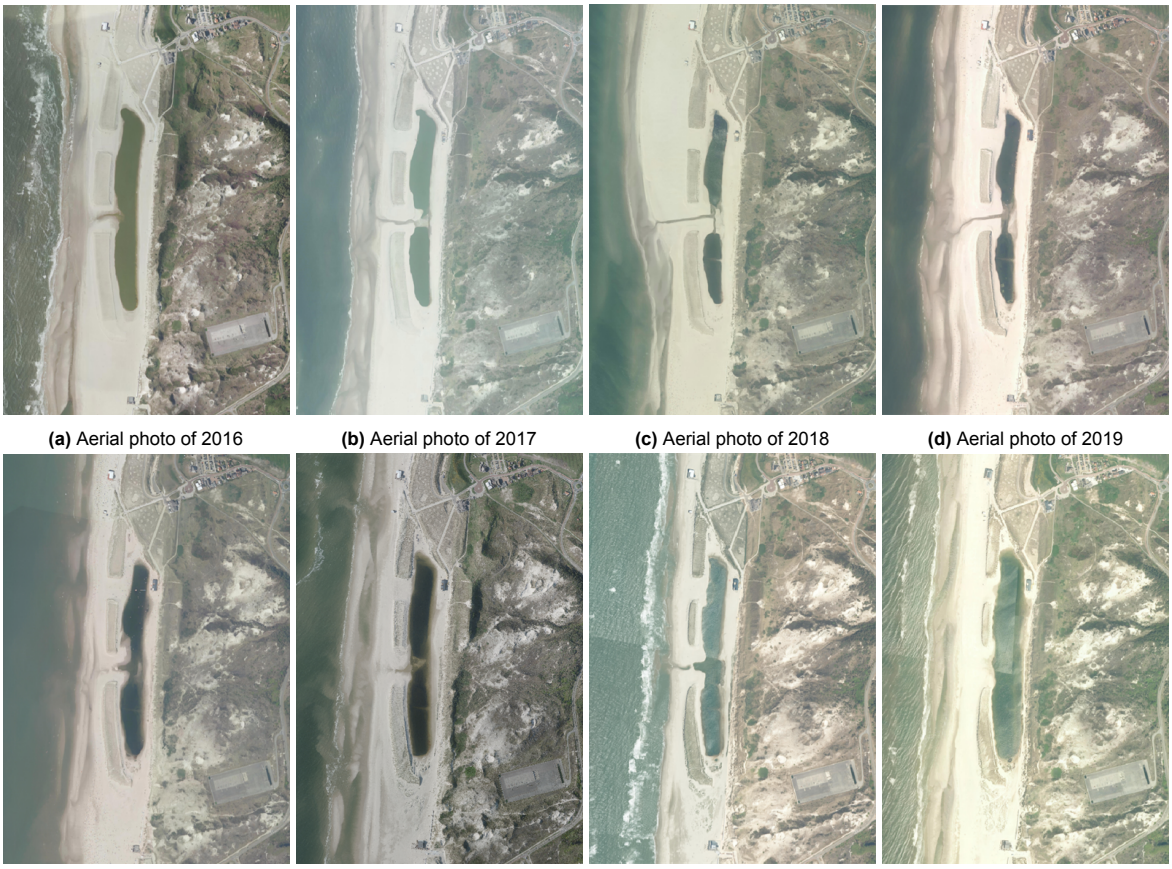

(a) Aerial photo of 2016 **(b)** Aerial photo of 2017 **(c)** Aerial photo of 2018 **(d)** Aerial photo of 2019

(e) Aerial photo of 2020 **(f)** Aerial photo of 2021 **(g)** Aerial photo of 2022 **(h)** Aerial photo of 2023

Figure 3.3: Aerial photos of the research area for the years 2016-2023. The photos have a resolution of 25 cm, except for the year 2021 which has a resolution of 8 cm. The photos are taken from Geotiles (GeoTiles & Rijkswaterstaat, 2023).

4

Methodology of detecting changes

In order to determine the change of the shape and size of the dunes, different methods can be used. These methods will be explained in the sections below. The methods considered are direct cloud to cloud comparison, cloud to mesh, multiscale model to model cloud comparison, k-means clustering, volume changes and the use of contour lines and cross sections. Multiple methods are used in order to find methods that work good for this data set.

The point cloud comparison methods and k-means clustering are pixel based methods. Being pixel based means that a specific point is tracked to see the changes over time. This only includes vertical movement that can be tracked. These methods are generally used to track areas that show a lot of change.

The methods of volume changes, contour lines and cross sections are object based. These methods track a specific object and see how this object changes over time. The object based methods can be used to see how the interesting objects, identified from the pixel based methods, change over time.

4.1. Data preparation

The lidar data downloaded (GeoTiles & Rijkswaterstaat, 2023), reaches from Hargen aan Zee in the south to Petten in the north. Since only the dunes surrounding the lagoon are studied, the data is cut to make processing faster. To show what the data looks like, part of the cut data (years 2016, 2019 and 2023) are shown in figure 4.1 with the scale in meters. By looking at these figures, it can be seen how the dunes change in general.

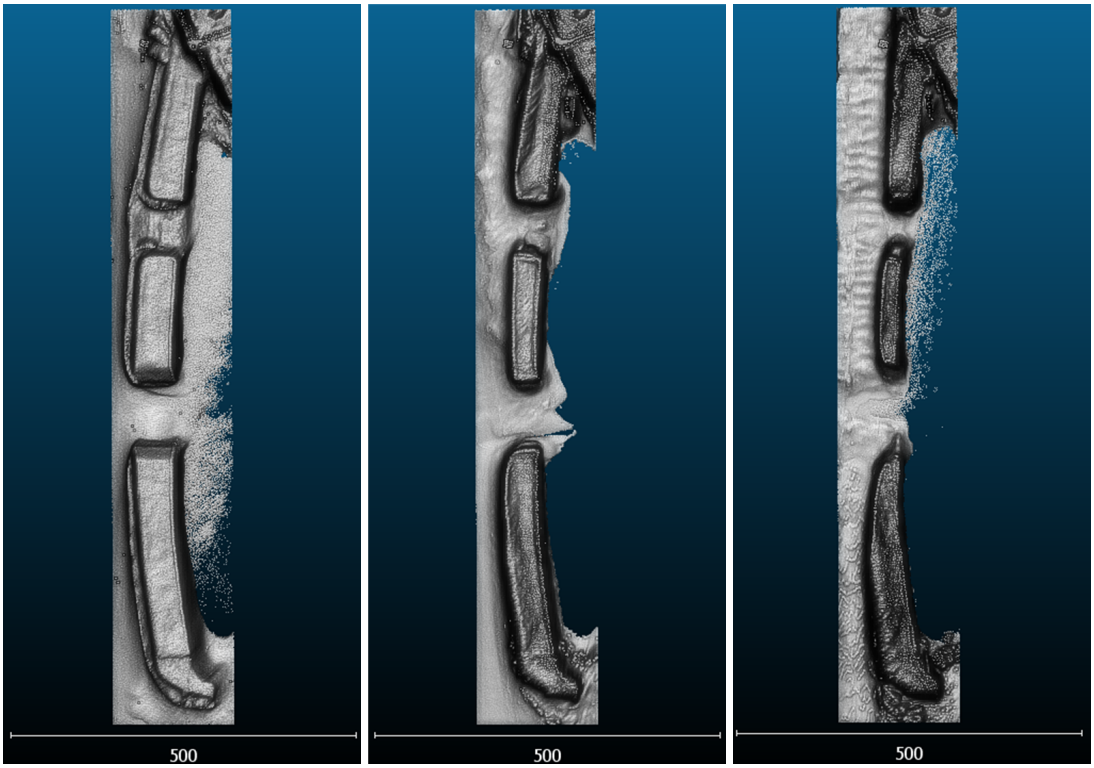

(a) 16-02-2016 **(b)** 24-02-2019 **(c)** 08-02-2023

Figure 4.1: Cut data of the years 2016, 2019 and 2023 shown in hill shade, the software Cloudcompare is used to visualise the data.

4.2. Methods of 3D point cloud comparison

Multiple methods exist to compare point clouds. The most common methods are Direct Cloud-to-Cloud comparison, Cloud-to-Mesh distance and Multiscale Model to Model Cloud Comparison. Each of these has been developed for their own purpose and detect different changes. All of them have been exploited in this study to see which one works best for this dataset. The point cloud comparison methods work in a 3D space and can detect distance changes between two data sets.

4.2.1. Direct Cloud-to-cloud comparison (C2C)

Direct Cloud-to-cloud comparison is one of the fastest and simplest methods of comparing 3D point clouds. For each point in a point cloud, the closest point in the other point cloud is found by nearest neighbor. The distance between the two points is used as the surface change. This method is very sensitive to outliers, point sampling spacing and surface roughness. It was developed for rapid change detection from dense point clouds (Lague et al., 2013).

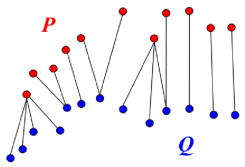

Figure 4.2: Direct Cloud-to-cloud comparison (Graves et al., 2022)

4.2.2. Cloud-to-mesh distance (C2M)

Another way of comparing point clouds, is the cloud-to-mesh distance. In this algorithm, the distance is calculated between a point cloud and a reference mesh (Lague et al., 2013). This method generally works good for a flat surface, where it is easier to create an accurate mesh.

In this study, a mesh is created from the point cloud of 2016 (figure 4.3). This is done by using the Delauney 2.5D (best fitting plane) in Cloudcompare. Following on this, the point clouds of the other years can be compared with this mesh to observe changes in the dunes.

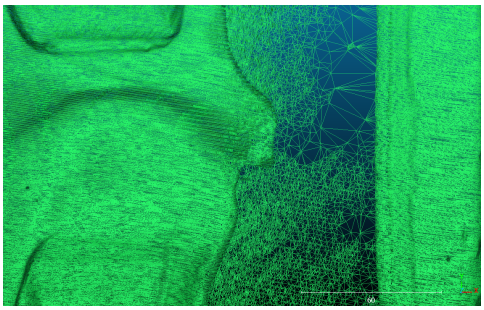

Figure 4.3: A zoom in of the mesh created from the point cloud of 2016. There is zoomed in on the part of the lagoon next to the channel.

4.2.3. Multiscale Model to Model Cloud Comparison (M3C2)

The Multiscale Model to Model Cloud Comparison (M3C2) is a more advanced model of comparing 3D point clouds. Corepoints are a selection of points of the reference cloud. Corepoints can be used to speed up the calculations. In this study, all points of the reference year (2016) are used as corepoints. First, a plane is fitted to a corepoint using the neighbours within a certain radius. From the fitted plane, the normal direction can be determined which is perpendicular to the fitted plane. Along the normal direction, a cylinder is defined with another certain radius. The axis of the cylinder passes through the corepoint and the length is defined (Lague et al., 2013). The cylinder intercepts with both clouds and this gives a subset of the top cloud and a subset of the bottom cloud. These are projected on the cylinder and this gives two distributions of the distances. From these, the mean is taken which is the average position of that cloud. Using both those average positions, the distance between the two clouds can be calculated (Winiwarter et al., 2021). The M3C2 algorithm only calculates a distance if there is an interception of the cylinder and the compared cloud (Lague et al., 2013).

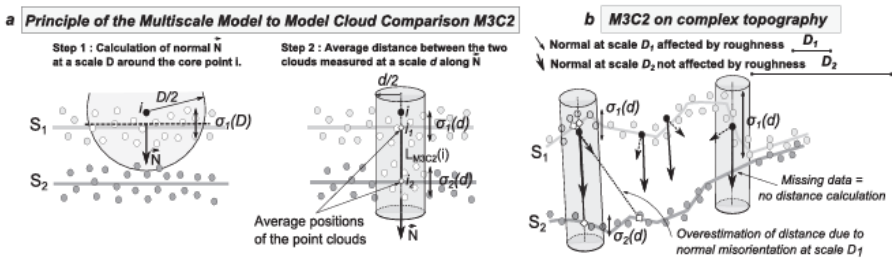

Figure 4.4: Description of the M3C2 algorithm (Lague et al., 2013)

For this algorithm, the two radii and the height of the cylinder can be set. For the M3C2 algorithm in Cloudcompare (Girardeau-Montaut, 2024), 1 meter is used for both radii (diameters of 2 meters). According to Actueel Hoogtebestand Nederland, 2019, the data will have at least one point per 2 m^2, which would make sure that for each point a plane can be fitted. The use of a larger diameter was tried but this had as a result that no details could be seen. A smaller diameter did also not increase the quality of the results. The height of the cylinder is defined to be 75.05 m.

4.3. Object based methods

The object based methods include volume changes and changes in 2D direction (cross sections and contour lines). The cross sections can give results of height and slope changes of the dunes, while contour lines show the change of shape of the dune over time.

4.3.1. Volume changes

To detect changes in the shape and the height of the dunes, the volumes of the dunes can be calculated. The areas of where the volumes are determined are shown in figure 5.7a. By calculating the volume change of the dune over time, a visual graph can be made to show whether the dune increases or decreases in volume and the dunes can be compared to each other.

The volume calculation is done in CloudCompare by computing the 2.5D volume. The year 2016 is again taken as the reference year and all the following years are compared with it. The volume is calculated for a grid. Since only a point cloud is available, a value for the empty cells is interpolated. A cell size of 1 meter is used for the calculation of the grid (Di Biase et al., 2021). The cell height gives the average height of all the points in that specific cell. After running the algorithm, the volume and surface change is given between two years. This change of volume can be plotted for each year to see how the dunes change over time and the dunes can be compared to each other.

4.3.2. Cross sections

Cross sections are made to observe the displacement of the dunes over time. It is a 2D method of detecting change. The cross sections show if the dune top and foot changes over time. For this, it is important to draw the cross section in the right direction in order to observe those changes. The cross sections are made in QGIS 3.34.7 'Prizren' (QGIS Development Team, 2023) using the Terrain profile plug-in.

4.3.3. Contour lines

Contour lines indicate points of equal elevation. These lines are used to see how the shape of the dune changes over time. If a part of the dune is eroded away, the height will have decreased there and the contour line will change shape.
The tracking of movement is split up in the dune foot, the middle of the dune and the dune top. These can be tracked using different contour lines of respectively 2.5, 3.5 and 4.5 meters. The contour lines are plotted in QGIS 3.34.7 'Prizren' (QGIS Development Team, 2023).

4.4. K-means Clustering

Many changes are expected to be found using the above described methods. Clustering can be used to find changes that are similar to each other. For this, k-means clustering will be used since it is an easy method to implement and was successful for similar studies on dunes (Lindenbergh et al., 2019). The objective is to form K amount of clusters, which is a number indicated by the user. First, an initial division is made with the K amount of clusters. Once all the points are assigned to a cluster, the initial center points are recalculated with the points in the cluster. Now, the process is done again and points are assigned to the new nearest cluster. The center point is again recalculated and this is repeated until a certain criterion is reached (Jin & Han, 2010). For this clustering method, the amount of clusters has to be given beforehand. For this study, the k-means clustering is done with k = 5, k = 6, k = 7, k = 8, k = 9 and k = 10. These clusters are based on a similar study of Lindenbergh et al., 2019 on clustering data of sandy beaches. Increasing the amount of clusters more made the graph difficult to interpret so it was decided to have a maximum of 10 clusters. To determine the optimal amount of clusters for classifying the dunes and the beach, the clustering is done with different amount of clusters for each run. All the different clusters are plotted to compare them visually.

The initial centers for k-means clustering are randomly chosen. The tolerance to have convergence is defined to be 0.0001. If the sum of squares within all clusters is smaller than this value, it is declared converged. If this does not happen, the maximum amount of runs is defined to be 300. The k-means clustering of time series in done in python using the py4dgeo package, version 0.6.0 (py4dgeo Development Core Team, 2022) and sklearn, part of the Scikit-learn package (Pedregosa et al., 2011).

Another way of seeing what the optimal amount of cluster is, is the elbow method. This is an empirical method which uses different amount of clusters to find the inflection point. This point is found using distortion. This is the average value of the squared distances from the cluster centers to the data points (Liu & Deng, 2021). The higher this value of distortion, the larger the variance within the clusters are.

5

Results

In this chapter, the results of the different methods for detecting changes in the dunes are discussed. First, the methods of 3D point cloud comparison are discussed in section 5.1. This section is subdivided to describe the three different methods: C2C, C2M and M3C2.
After this, the object based and 2D change methods are discussed in section 5.2. The volume changes of the dunes, the cross sections and the results of contour lines are discussed here.
Lastly, the clustering of the results is done in section 5.3 by k-means clustering.

5.1. Methods of 3D point cloud comparison

The methods of C2C, C2M and M3C2 are used to detect 3D changes in the area. For each method, the distances are shown in sub-figures which represent the distance changes between the reference year 2016 and the to be studied year. The results for the C2C, C2M and M3C2 methods are shown in figures 5.1, 5.2 and 5.3 respectively.

To quantify the changes, histograms can be made for the different methods of point cloud comparison. These histograms represent the distance changes between 2016 and 2023 to see how the study area changed from the beginning of the data to the end of it. The distance changes from -4 to +5 meters are shown. The changes outside of this range were so limited that they were not visible in the histograms.

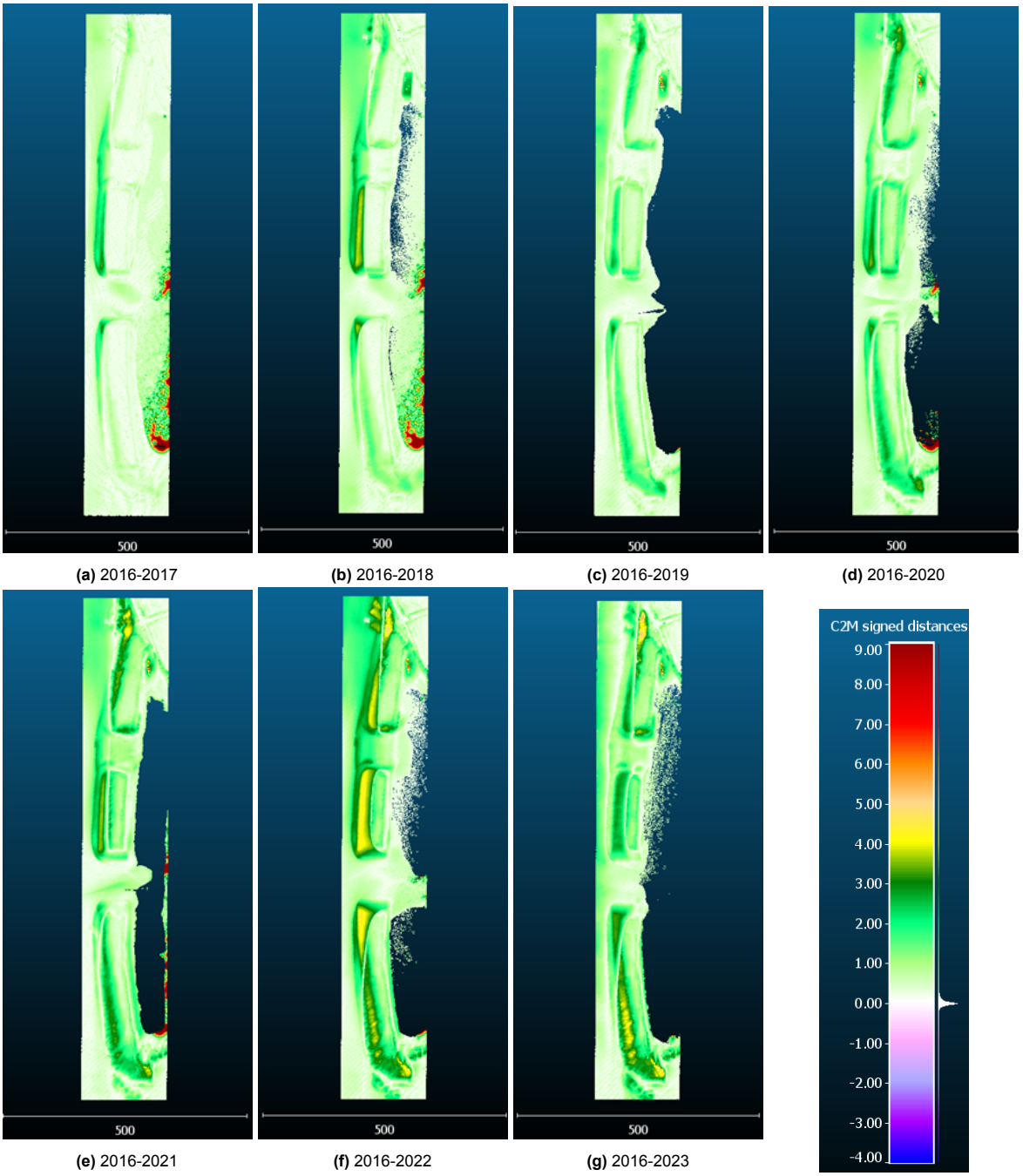

(a) 2016-2017 **(b)** 2016-2018 **(c)** 2016-2019 **(d)** 2016-2020

(e) 2016-2021 **(f)** 2016-2022 **(g)** 2016-2023

Figure 5.1: C2C distances for the years 2017 to 2023, compared to the reference year 2016. The distances are in meter.

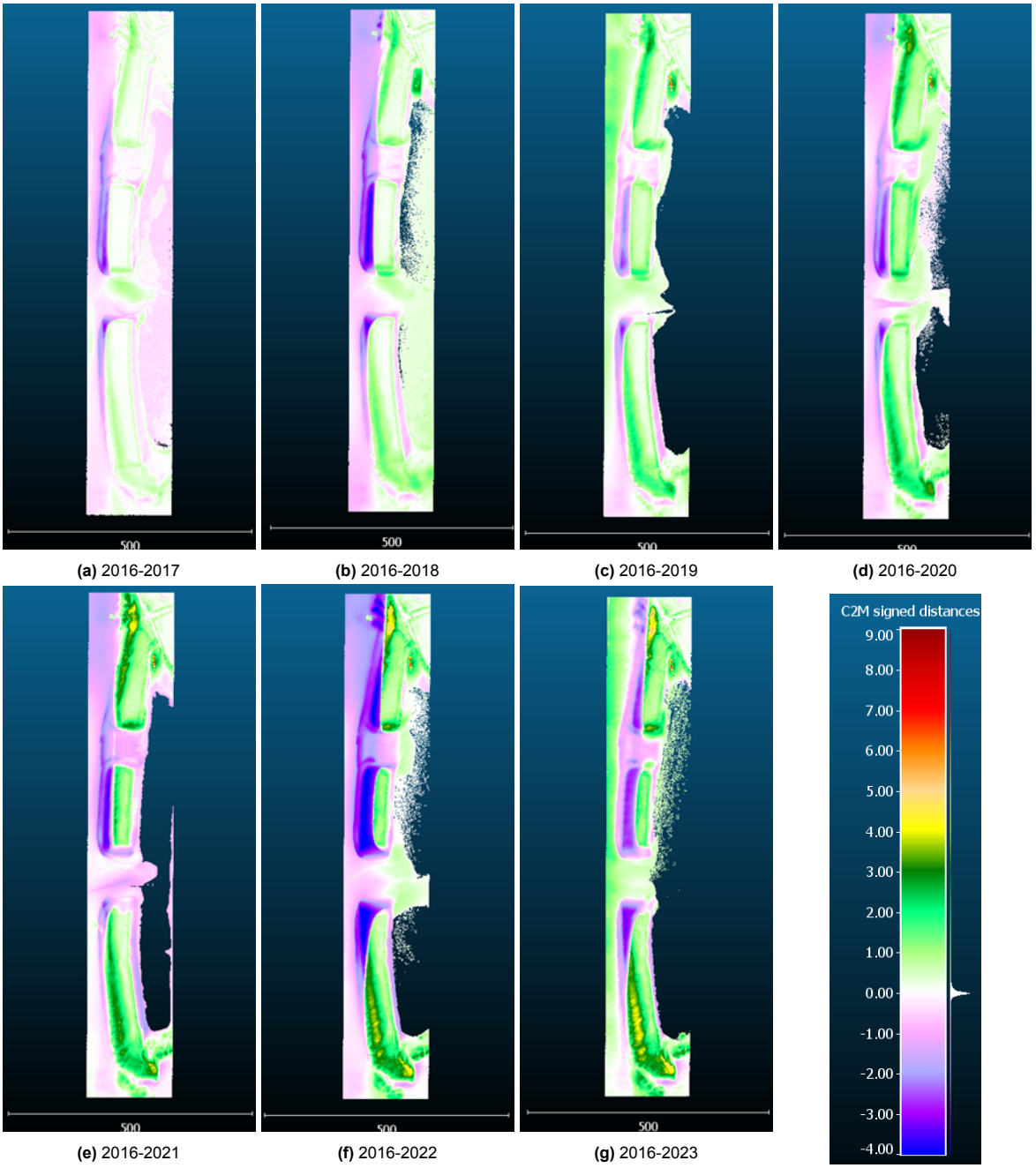

(a) 2016-2017 **(b)** 2016-2018 **(c)** 2016-2019 **(d)** 2016-2020

(e) 2016-2021 **(f)** 2016-2022 **(g)** 2016-2023

Figure 5.2: C2M distances for the years 2017 to 2023, compared to the reference year 2016. The distances are in meter.

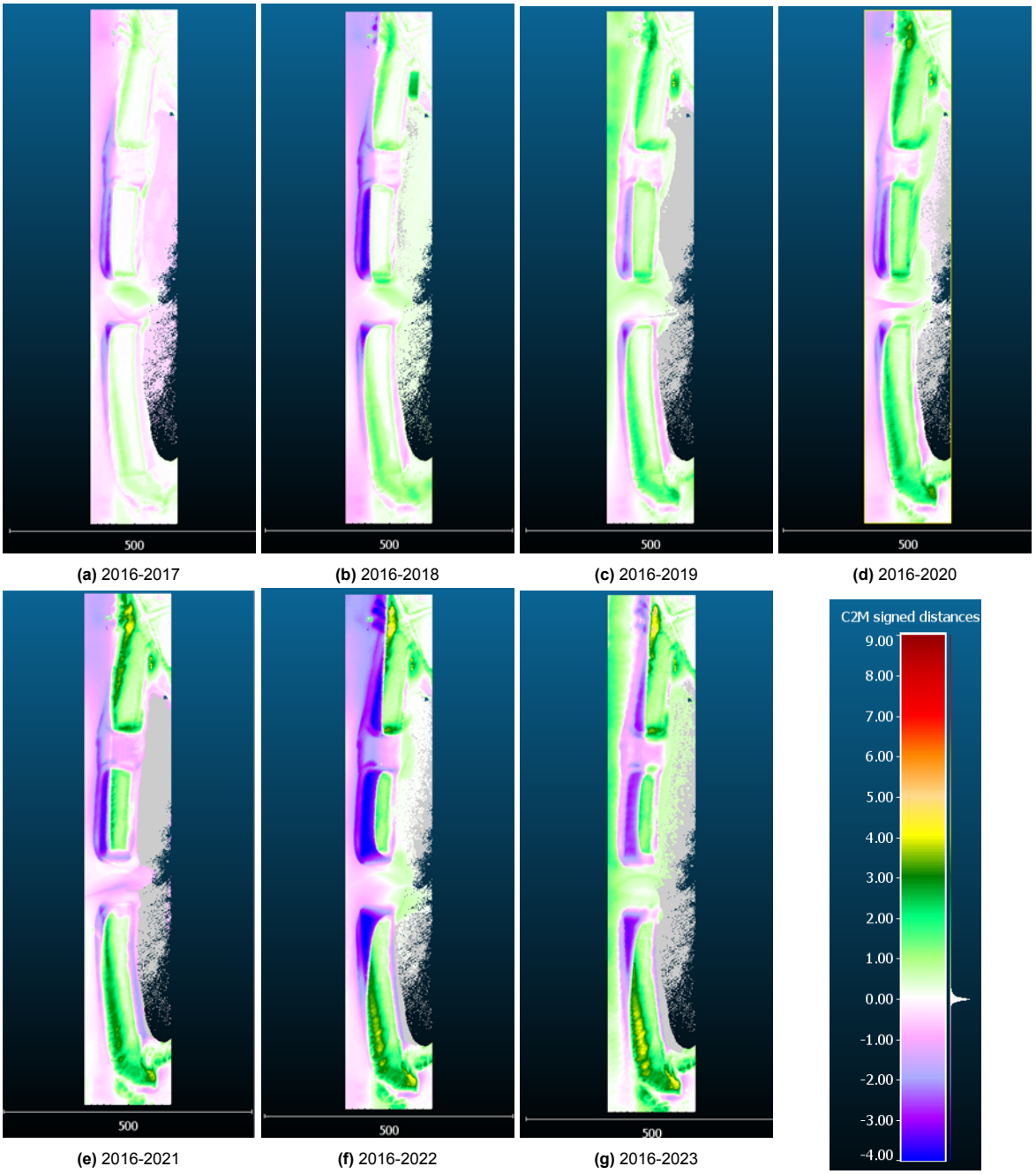

(a) 2016-2017 **(b)** 2016-2018 **(c)** 2016-2019 **(d)** 2016-2020

(e) 2016-2021 **(f)** 2016-2022 **(g)** 2016-2023

Figure 5.3: M3C2 distances for the years 2017 to 2023, compared to the reference year 2016. The distances are in meter.

5.1.1. C2C

As observed in figure 5.1, the C2C method only shows absolute distances. This means that no interpretation can be made whether a specific part has been subjected to erosion or deposition. It does highlight regions with a lot of change.
These regions are the southern part of dune 3, the northern part of dune 1 and the west part of dune 2. In 2022, there is a change of around 4 meters on the seaside of the dunes.

In figure 5.4, the histogram of the C2C distances is shown. It is seen that the distances are all positive because of the absolute distances. Also no changes of 0 meter are observed with this method.
The time to compute the C2C distances between the reference year and any other year is around 3 seconds.

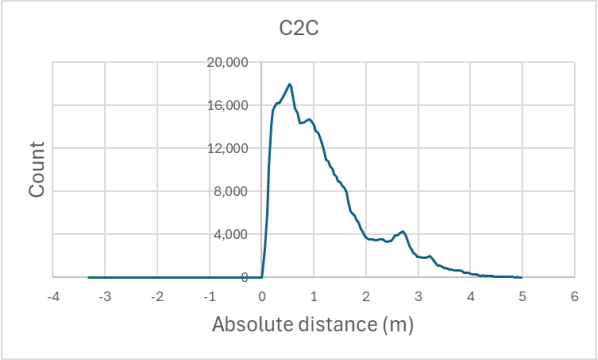

Figure 5.4: Histogram of the C2C method for the changes between 2016-2023

5.1.2. C2M

From the results in figure 5.2, it is seen that there is a difference between erosion and deposition. In all the years, there is erosion on the west side of dune 2, a maximum of 4 meters in 2022 compared to 2016. In this year, this amount of erosion is also seen at the sides of dune 1 and 3. After this year, the height is increased by 1 meter again on all those locations. The height of the east side of the dune does increase by 2 meters between 2016 and 2023.
The northern side of dune 1 and the southern side of dune 3 only show signs of deposition. Even in the year with a lot of erosion (2022), the height of these spots is increased. South of dune 3, there is a constant increase in height over the years.
A sharp increase in height is seen in the north east corner of dune 1. This is an increase of between 5 and 9 meters.

The histogram of the C2M distance changes between 2016 and 2023 does show positive and negative values. A lot of pixels have a distance of 0.5 meters. These are mainly the points in the lagoon and on the north of the dunes.
The time to compute the C2M distances between the reference year and any other year is around 30 seconds.

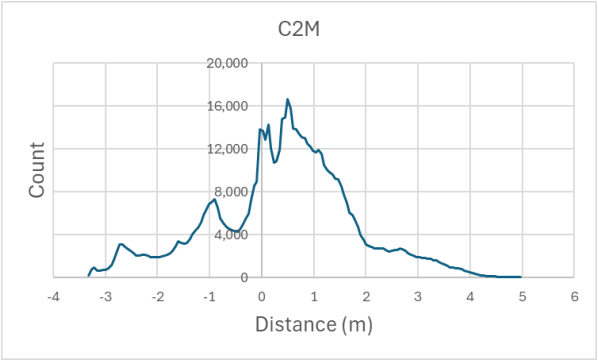

Figure 5.5: Histogram of the C2M method for the changes between 2016-2023

5.1.3. M3C2

The results obtained using the M3C2 method (figure 5.3) look similar to the results of the C2M method, but a big difference is the magnitude of the distance changes. For the M3C2 method, the maximum distance change detected is 5.5 meters, while for the C2M the maximum distance is 9 meters. This difference is the case in the northeast corner of dune 1. Also the other increases in height are less extreme for the M3C2 method.

A sharp peak at 0.5 meters is seen in the histogram of the changes between 2016-2023 according to the M3C2 method (figure 5.6). These are mainly the distances changes of the points within the lagoon. The shape of this histogram is similar to the C2M method, but a smaller amount of higher distances

are present in this method. For example, the M3C2 method detects approximately 1000 changes of 3 meter, while the C2M method detects around 2000 changes of this same distance. The extreme values are more averaged out in this method.
The time to compute the M3C2 distances between the reference year and any other year is around 20 seconds.

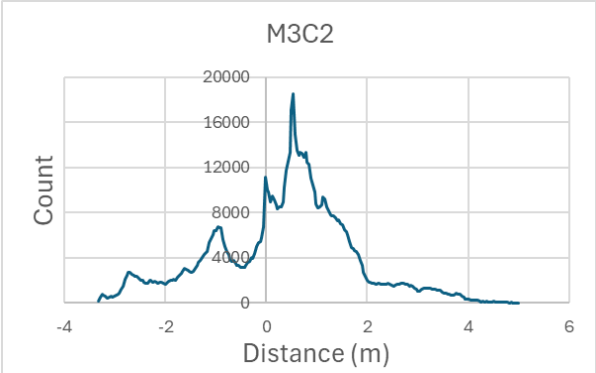

Figure 5.6: Histogram of the M3C2 method for the changes between 2016-2023

5.2. Object based methods

The object based methods are used to look at the volume changes of the three dunes separately and any changes in the 2D direction using cross sections and contour lines.

5.2.1. Volume changes

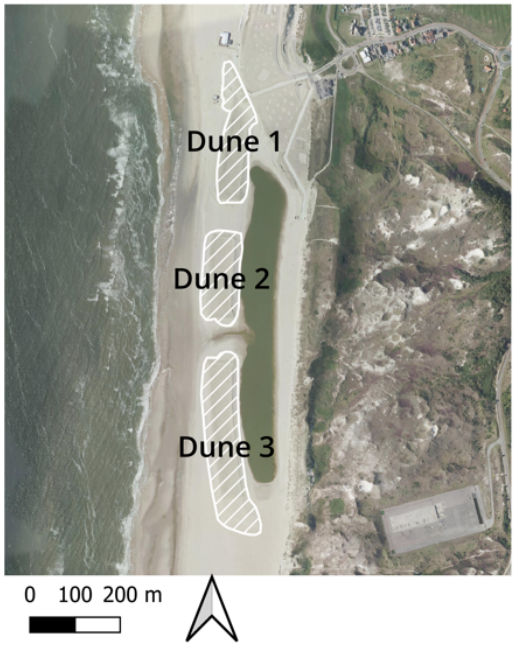

(a) Locations of the three dunes which are observed for volume changes

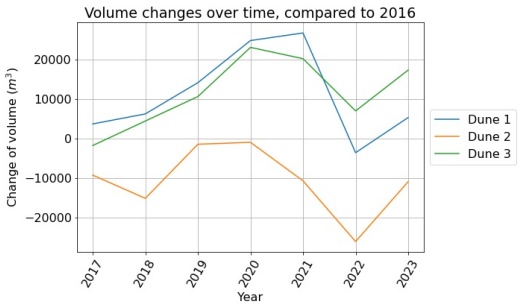

(b) The volume changes of the three dunes, all compared to the starting year 2016

Figure 5.7: Volume changes for the three indicated dunes, compared to the year 2016

The different dunes experience different amounts of erosion and deposition. The volume changes of the dunes are calculated to see if the entire dune grows or shrinks over time. In figure 5.7a, the division of the three different dunes is shown. The volumes changes calculated for dune are shown in figure

5.7b. The volume changes are given in m^3 compared to 2016.

Dunes 1 and 3 show a gradual increase in volume over the years. Only in 2022 there is a large decrease compared to the years before. Dune 2 decreases in volume over the years with the greatest decrease in 2018 and 2022. It does show a relative increase in volume in 2023, compared to 2022. From the volumes, it can be seen that dune 3 is the least eroded over the years.

5.2.2. Cross sections

On several locations, shown in figure 5.8, cross sections are made to see how the shape and height of the dunes change over the years, and especially the location of the dune top. It is chosen to make cross sections through each of the three dunes, and two through dune 3 since that dune has the largest spatial variability. Two other cross sections are made parallel through the dunes, to see how the height and the channel change. The cross sections can be found in figure 5.9.

Figure 5.8: The six locations where the cross sections are taken. Other cross sections are taken through the channel from north to south and through the opening in the north, from north to south as well.

Cross section 1 and 3 look similar to each other. The overall trend is that the height of the dune top increases each year by 0.5 meter. Then suddenly in 2022, the peak of the dune changes place by approximately 10 meters and the slope gets steeper. After this event, the overall trend continues and the height increases in 2023 compared to 2022. In cross section 4, the height also increases each year by 0.5 meter, but it does not change place in 2022.
Cross section 2 goes through dune 2 which has been determined as the dune with the most changes by the previous methods. Also in the cross sections it is seen that the location of the dune top changes each year. It is also the lowest dune in height of the three.

The cross sections 5 and 6, which are parallel through the dunes and the channel / openings, are more difficult to interpret. It is seen that the overall height of the dunes does increase over the years. The behaviour of the channel and the north opening can be studied by the cross sections as well. The level of the north opening varies through the years, but the main trend is a decrease in height. The level of the channel also seems flat for most years. In 2020 there is a clear channel present.

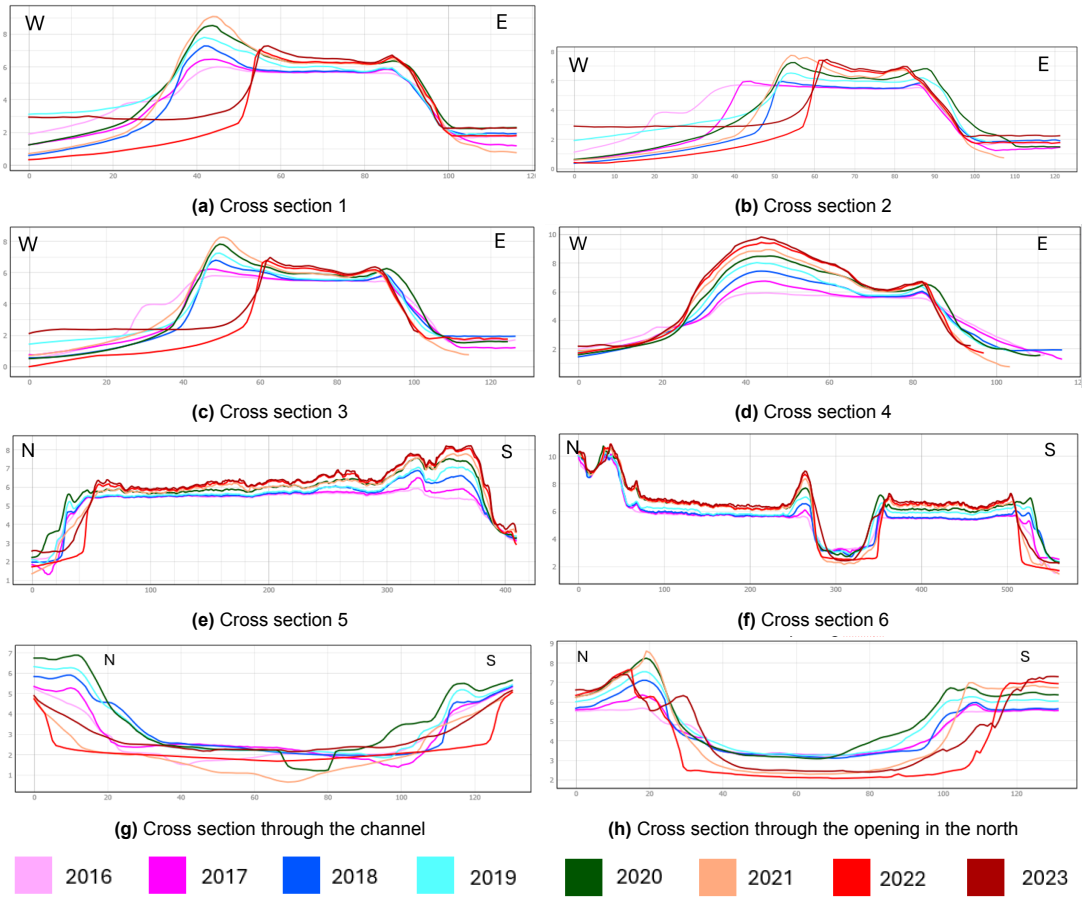

Figure 5.9: Cross sections at the eight locations through the dunes, channel and opening in the north.

5.2.3. Contour lines

Contour lines can be used to see how the shape of the dune changes over time. The plots which visualize the moving of the contour lines over the years are shown in figure 5.10. When looking at the highest contour (figure 5.10c), it is seen that the dune top gets smaller over the years. The lower contour line of 2.5 m (figure 5.10a) shows more variation through the years. In 2019 and 2023, the contour line is more towards the sea than in the others years.

It is clearly shown how the sides of the dune change shape over time. The dunes were originally formed with square sides. Over the time these are rounded as this is a more natural form.
It is also seen that there is some sort of activity present in the northeast corner of dune 1 from 2018 on. This was also already seen in the point cloud comparison methods by detecting a sharp increase in height.

In the south of dune 3, it is also seen that much change is happening when looking at the contour lines of 3.5 and 4.5 meters. When looking at the aerial photos, this could indicate on the formation of new dunes. However, this is outside the scope of this study and will not be further discussed.

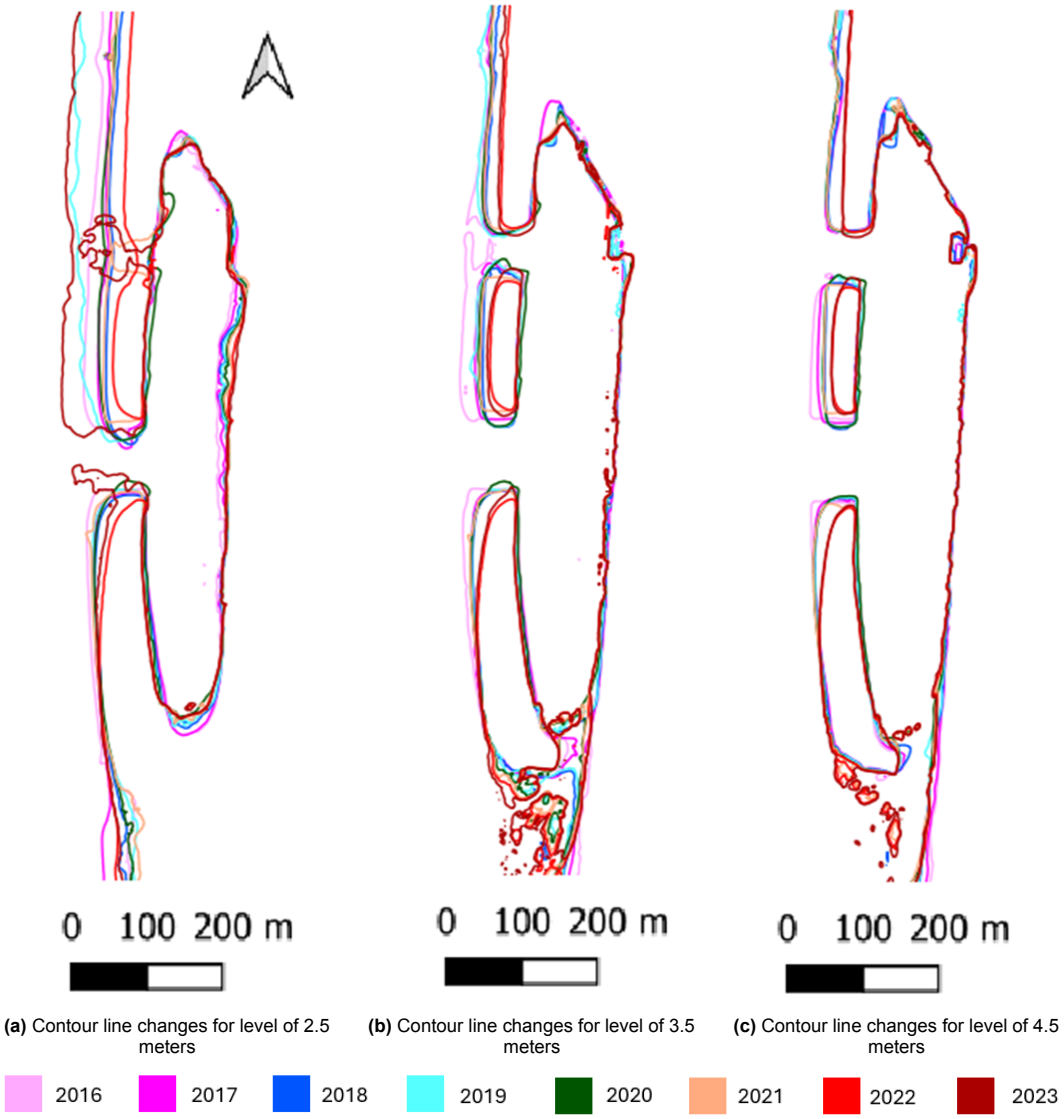

(a) Contour line changes for level of 2.5 meters **(b)** Contour line changes for level of 3.5 meters **(c)** Contour line changes for level of 4.5 meters

Figure 5.10: The contour level changes of the years 2016 to 2023 for different levels.

5.3. K-means clustering

The changes detected by the methods of point cloud comparison (C2C, C2M and M3C2) can be clustered using k-means clustering. The changes that are similar to each other will be added to the same cluster and the time line of these changes is shown as how the average of each cluster behaves over time. The clustering with different amount of clusters is shown in figure 5.11.

With 5 clusters, no cluster is present which represents areas with almost no change. In the methods of point cloud comparison, it is seen that many areas do change but only by a small amount (0.25 meters). This is better clustered by using more than 5 clusters.
By using 6 clusters, a cluster is added which represents the small changes on the beach.
In the clustering done with 7 clusters, it is noticed that the opening in the north is clustered differently than with the previous amount of clusters. It is now clustered as having a decreasing height over time, instead of approximately constant. This is the same result as using the point cloud comparison methods and the cross sections through the opening.

The clustering with 8 to 10 clusters is very detailed. Multiple clusters are defined for pixels that increase in height. It shows differences in how the height of the east side of dune 2 changes, while it was determined constant in the previous methods. This makes that 8 clusters and more provide too much

detail for this study.

Considering all these factors and studying all the graphs with different clusters, it is determined that the changes are best clustered by using 7 clusters. This gives a detailed clustering, but does not overfill.

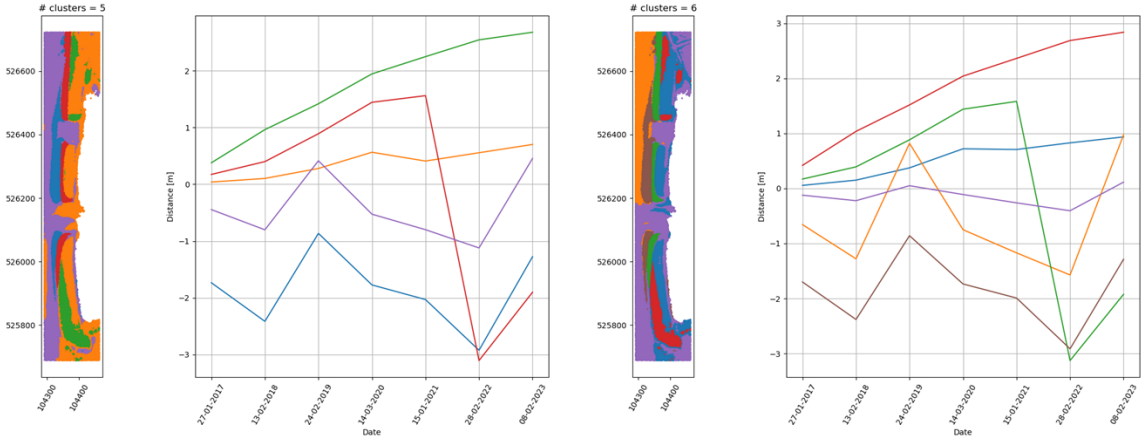

(a) K-means clustering done with 5 clusters.

(b) K-means clustering done with 6 clusters.

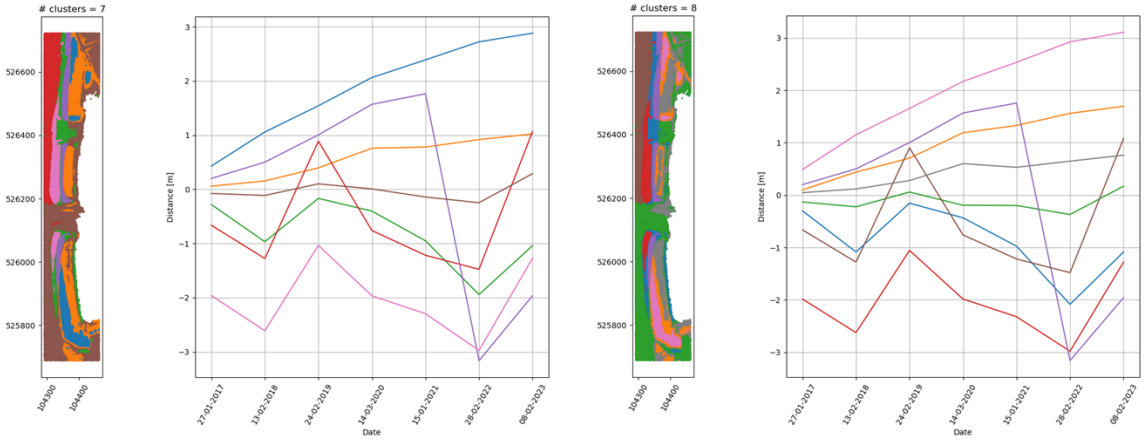

(c) K-means clustering done with 7 clusters.

(d) K-means clustering done with 8 clusters.

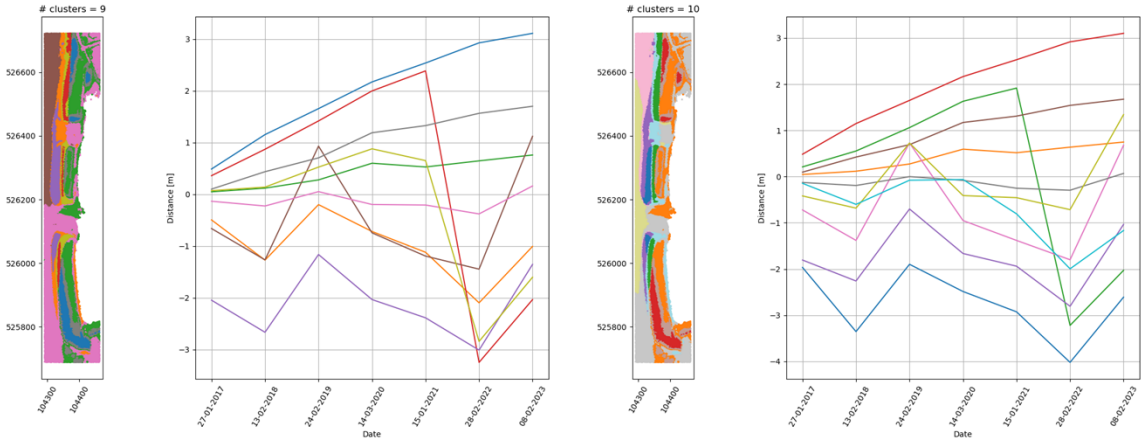

(e) K-means clustering done with 9 clusters.

(f) K-means clustering done with 10 clusters.

Figure 5.11: K-means clustering results. The time series locations are colored by cluster. In the graphs of each sub-figure, the median of all time series belonging to that cluster is shown. The colors in the time series plots correspond to those in the spatial plots. The colors are not the same in each sub-figure.

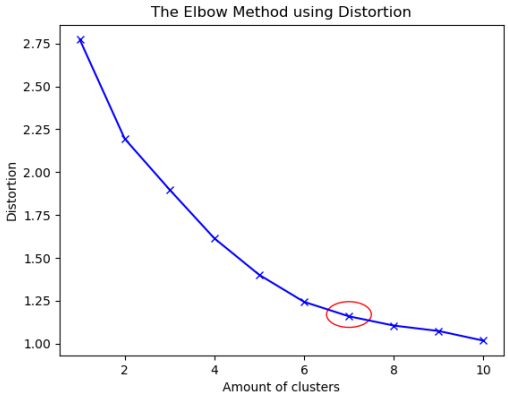

Figure 5.12: Graph of amount of clusters plotted against the distortion for k-means clustering.

The elbow method, described in section 4.4, is used to validate the amount of clusters chosen. The result is shown in figure 5.12. Distortion is the average value of the squared distances from the cluster centers to the data points. If this value is low, this means that the squared distances are smaller and therefore the points are more similar to the cluster centers. For the addition up to 7 clusters, the distortion largely decreases, which indicates that the clustering gets much better with more clusters. After 7 clusters, the steepness of the line decreases, which means that the addition of clusters does not add much value to the quality of the clustering. This point is the inflection point and is for this data at 7 clusters.

By comparing different amount of clusters and using the elbow method, it is determined that 7 clusters works best for this data set and study.
Looking at figure 5.13 (which shows k-means clustering with 7 clusters), the clusters detected can be compared and linked to the changes found using other methods discussed.
The majority of the dunes is colored orange. This indicates a steady increase of a total of 1 meter over the years. This corresponds to the findings of the point cloud comparison methods, except that the value there was slightly higher (2 meters). The blue color shows that the northern part of dune 1 and the southern part of dune 3 increase more than the rest of the dunes (0.6 meter per year). The northeast spot of dune 1 is also included in this cluster, while in the other methods a distance change of 9 meters was found.
The green color is mainly present in the northern opening. At this spot, the height decreases over time, just as seen in the cross sections. The purple cluster shows a big increase of height up to 2021 and after this a decrease in height of 4.5 meters between 2021 and 2022. This is the same erosion found as in the C2M and M3C2 method on the seaside of all three dunes. Between 2022 and 2023, this part grows with a higher rate than before, 1 meter per year.
The brown cluster does not show big changes, also for the channel in the south opening. The red and the pink cluster are only present outside the dunes and are therefore not considered.

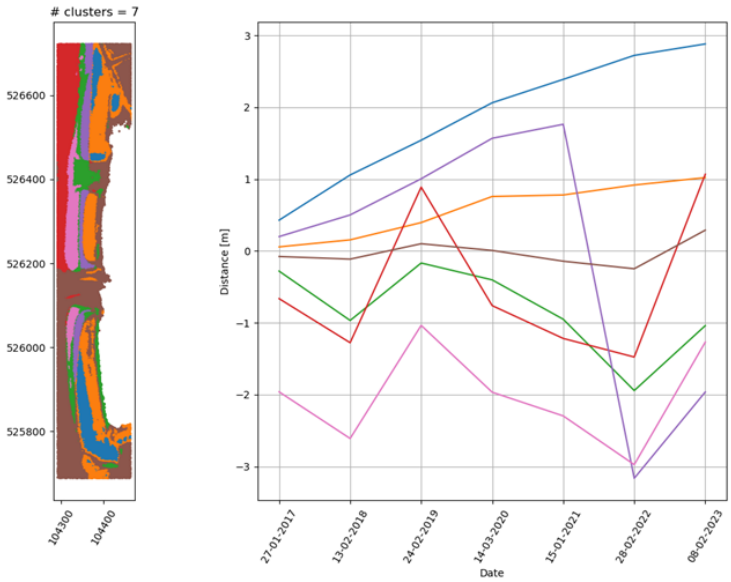

Figure 5.13: K-means clustering done with 7 clusters

6

Discussion

This chapter will start with section 6.1 where some of the results are interpreted and a comparison to other studies are made. After this, the methods are compared in section 6.2 and limitations of the data set are discussed in section 6.3.

6.1. Interpretation of the results

Using all results from the methods discussed in the previous chapters, an interpretation can be made on what happened in the dunes during the years 2016-2023.

The lagoon side of the dunes increases steadily in height with a rate of 0.5 meter per year. This is since no marine erosion has taken place and aeolian transport indicates positive growth (de Vries et al., 2012). The rate of 0.5 meter increase per year is also found on the dunes near Noordwijk by Vos et al., 2024.

Heavy erosion is seen on the west side of the dunes protecting the lagoon due to the storm in 2022. By this erosion, the dune top is moved approximately 10 meters land inwards. A comparable amount of dune retreat is found due to other storms (Van Wiechen et al., 2023). The volume of the three dunes has increased from 2022 on. This was done by the placement of screens of natural material (figure 6.1) to make sure the dunes do not disappear. Since no data is available from 2024, it is unknown dune 2 is still growing or if it is shrinking again.
Dune 2 shows more erosion since is it less vegetated compared to the others, especially the north of dune 1 and the south of dune 3. The difference in vegetation is seen in the aerial photos.
Dune 2 has openings on both the south and north side. It is possible that the sea and humans cause more erosion here.

Other features that are present in the results are the channel which leads to the sea and an anthropogenic change.
The channel is only visible in 2020. It is most probable that the dredging had just occurred before the data was taken. This is since the data of 2020 is taken in March, which is later in the year than for the other years. The channel is dredged in the spring before the recreational season. For the other years, the level of the channel slightly varies.
In the C2M plots, a sudden increase of height was seen in the north-east corner of dune 1. This is the building of a playground in 2018 (figure 6.2).

Figure 6.1: Screens made from natural material found on the sides of the dunes. Picture taken by the author on June 5th, 2024.

Figure 6.2: A playground built in 2018. The height increase was seen using the different methods.

6.2. Comparison of methods

The methods of C2C, C2M and M3C2 are used to detect 3D changes in the area.
C2C has proven to be a very fast method with low computational time, but does not show the difference between deposition and erosion since it only calculates the absolute distance between two point clouds. Since the points are not on the same location in all the point clouds, the C2C method cannot compare them well. This is seen in the histogram (figure 5.4) as no distances of 0 meters are observed.
Overall, this makes that C2C is not a useful method for this study.

The C2M and M3C2 methods show similar results. They both show the difference between erosion and deposition and the computational time is approximately the same. However, in figures 5.2 and 5.3, it is seen that the M3C2 distances give less detail and extreme values are less present in M3C2 than in C2M. A zoom on dune 1 is given in figure 6.3. The building of the playground is clearly shown by the C2M, but only vaguely with the M3C2 method.
This is since the M3C2 method uses neighbors in an area around the point with diameter of 2 meters to find the fitted plane and therefore the normal direction. The playground is a very small area with only a few points with this large height. These values will be averaged out with the M3C2 method. This makes that not many details can be seen. For the C2M method, a very detailed grid can be made since the point density is high. This makes that the playground can be seen in the C2M plots better than in the M3C2 plots.
This is the same case for the histograms (figures 5.5 and 5.6). The extreme values are average out in the M3C2 method, while they are visible in the C2M method.

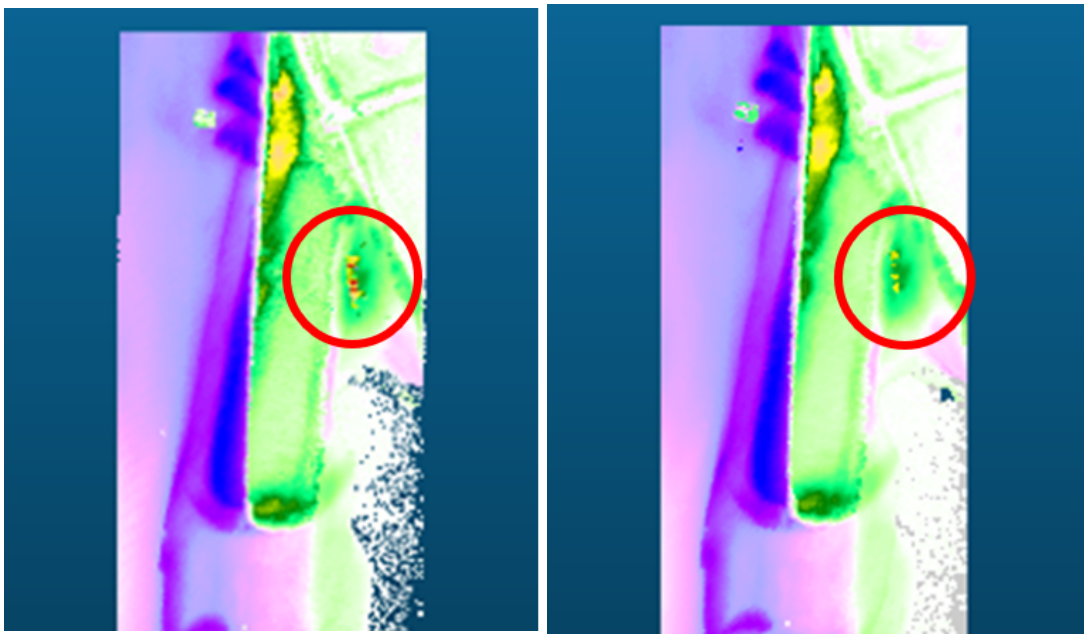

(a) The C2M method for dune 1, comparison between 2016 and 2022

(b) The M3C2 method for dune 1, comparison between 2016 and 2022

Figure 6.3: Comparison between the C2M and M3C2 method for dune 1, comparing the years 2016-2022.

For the method of detecting volume changes, only the separate volumes of each of the three different dunes were taken into account. If the volume moved outside the selected area of the dune, this is not integrated in the calculation. It could be looked at with a larger area and see how it changes within.
The methods of cross sections and contour lines worked well to detect changes in the height and shape of the dunes. The contour lines show also the formation of new dunes in the south of dune 3. This indicates that the use of contour lines would be a good method for detecting the growth of new dunes.

Regarding k-means clustering, a disadvantage of this method is that the amount of clusters has to be defined before running the algorithm. To compensate for this, the algorithm was done with 6 different amount of clusters. It is difficult to quantify what the optimal amount of clusters is for a certain study

area. It was chosen to use 7 clusters, but using more or less clusters can also have advantages. This is partially personal preference. To eliminate this element, it could be checked if there is another suitable clustering method where the amount of clusters do not has to be specified beforehand.

6.3. Limitations of the dataset

The data is not recorded on the same day of each year. This is since it is undesirable that the data is influenced by clouds and the data is recorded by low tide. It does makes it harder to compare two years with each other. This is mainly seen by the data set of 2020, which is taken in March, while most others are taken in January and February.

Next to this, there are a few gaps in the data set. This is due to the fact that points can only be partially obtained if there is a surface with water on it. This is the case for the area of the lagoon. That is the reason why for some of the methods the distances are also computed for the lagoon, and for some not. Since the lagoon is not the goal of this study, this is not a big limitation. If it is desired to extend the study area, this is an important factor to keep in mind.

7

Conclusion

In this chapter, a final conclusion will be drawn. This is done by answering the research questions posed in the introduction. The answers can be found in section 7.1. Recommendations are given in section 7.2.

7.1. Answering the research questions

The dunes protecting the lagoon from the sea have changed a lot over the years 2016 to 2023. This research aimed to answer several question. First, the sub-questions are answered and after this, an answer is given to the main research question.

How is lidar data obtained and how can it be used to quantify changes?
Lidar data is obtained by airborne laser scanning. The JARKUS data is a yearly coast measurement which determines the coast line of the Netherlands. Only the laser measurements on the dry parts are used for this study from the years 2016-2023. This data set exists of 3D point clouds for each year. The year 2016 is used as the reference in this study. The point clouds contain height information about all the points. These heights can be compared to each other using several different methods such as C2C, C2M, M3C2, volume changes, cross sections, contour lines and k-means clustering, implemented in software such as Python, CloudCompare and QGIS.

What are good methods of detecting changes in the dunes?
Considering all methods used, C2M is considered to be a good method to detect 3D changes. These changes can be clustered by k-means using 7 clusters for this area. Volume changes show how much the dunes change, but do not show where the dunes change exactly. Contour lines and cross sections work well for detecting 2D changes.

Where do the greatest changes occur in the dunes?
The greatest changes occur on the west side of dune 2, the north of dune 1 and the south of dune 3.
The west side of dune 2 experiences 4.5 meters erosion in 2022 due to a storm, which makes that the dune top moves 10 meter land inwards. This part does show a higher grow rate in 2023 again (1 meter per year).
The top of the dunes grow with a rate of 0.5 meter per year. The north of dune 1 and the south of dune 3 grow with the same rate, but do not show any signs of erosion which makes that the overall height is higher.
Overall, dune 1 and 3 increase in volume, except in years with heavy erosion, while dune 2 decreases most years in volume.

How can changes of the shape and the height of the dunes protecting the lagoon at Camperduin from the sea be detected using annual lidar data from 2016 tot 2023?
The changes of the shape and the height of the dunes can be detected using annual lidar data. The lidar data is obtained as point clouds and these can be compared with each other by using the C2M method together with k-means clustering, volumes, cross sections and contour lines.

To a certain extent, it is possible to predict the future of the dunes how they will develop. However, as seen in the results, weather events have a big influence on the dunes. This makes it difficult to draw any definite conclusions of what will happen to the dunes in the future.

7.2. Recommendations

Below are given some recommendation for further research. The recommendations are subdivided in additional methods and improvements, other changes in the study area and extension of the study area.

Additional methods and improvements

- In this study, the unit for volume changes of the dunes was m^3 / year. In other studies the dune volume change is given in m^3 / m / year. If the volumes obtained in this study could be converted to the same units, it would be easier to compare.
- Another 3D point cloud comparison method is the mesh-to-mesh method. This method is not considered in this study due to limitations in time. It would be interesting to see how this method differs from the C2M method.
- More seasonal changes could be detected by using radar satellite data. This is available more regularly. This would be available on the website of the Netherlands Space Office (NSO, n.d.).
- Another clustering method can be used. This would be useful since the amount of clusters defined from k-means clustering is also partial personal preference. Another clustering method that does not require the amount of clusters to be defined before hand is hierarchical clustering (Rokach & Maimon, 2005).

Other changes in the study area

- It was seen that smaller dunes were developing in the south of the study area. Another study could be done to see how these dunes develop and which methods work good to quantify changes on growing dunes, instead of already existing dunes as for this study.
- Some changes in the intertidal zone were also seen in the study area. A smaller timescale would be needed to quantify these changes.

Extension of the study area

- It can be investigated if the same methods also work for other dune areas and what happens if the study area is increased in size, for example the entire Hondsbossche Dunes or the entire coast of the Netherlands.

References

Actueel Hoogtebestand Nederland. (2019, July). *Besteksvoorwaarden inwinning Hoogdynamische gebieden AHN 2020-2022* (tech. rep.).

Bodde, W., Huiskes, H., IJff, S., Kramer, H., Kuiters, A., Lagendijk, G., Leenders, J., Ouwerkerk, S., Scholl, M., Smit, M., Smits, N., Stuurman, R., van der Valk, B., Verheijen, A., de Vries, D., & Wegman, C. (2019). *Innovatieproject Hondsbossche Duinen: Eindrapportage, definitief 01*. Ecoshape.

de Vries, S., Southgate, H., Kanning, W., & Ranasinghe, R. (2012). Dune behavior and aeolian transport on decadal timescales. *Coastal Engineering*, *67*, 41–53. https://doi.org/https://doi.org/10.1016/j.coastaleng.2012.04.002

Deltares. (2019, May). Zwakke schakels. https://publicwiki.deltares.nl/display/KWI/2.3.1.01.+Zwakke+schakels+-+algemeen

Di Biase, V., Hanssen, R. F., & Vos, S. E. (2021). Sensitivity of Near-Infrared Permanent Laser scanning intensity for retrieving soil moisture on a coastal beach: calibration procedure using in situ data. *Remote sensing*, *13*(9), 1645. https://doi.org/10.3390/rs13091645

Ernstsen, V., Winter, C., Bartholomä, A., Flemming, B., & Bartholdy, J. (2007). Calculation of bedload transport in a tidal inlet channel based on high-resolution, high-precision multibeam echosounding.

Gemeente Schagen. (2024, May). Recreatiestrand Hondsbossche duinen voorlopig behouden. https://www.schagen.nl/recreatiestrand-hondsbossche-duinen-voorlopig-behouden

GeoTiles & Rijkswaterstaat. (2023). Readymade geodata with a focus on the Netherlands. https://geotiles.citg.tudelft.nl/

Girardeau-Montaut, D. (2024, March). CloudCompare. https://www.cloudcompare.org/

Graves, W., Aminfar, K., & Lattanzi, D. (2022). Full-scale highway bridge deformation tracking via photogrammetry and remote sensing. *Remote Sensing*, *14*, 2767. https://doi.org/10.3390/rs14122767

Harikumar, A. (2020, June). *Advanced methods for tree species classification and biophysical parameter estimation using crown geometric information in high density lidar data* [Doctoral dissertation]. https://doi.org/10.13140/RG.2.2.10395.69922

HKV. (2020, September). Building with Nature. https://www.hkv.nl/projecten/building-with-nature/

Hoogheemraadschap Hollands Noorderkwartier, Rijkswaterstaat, van Oord, & Boskalis. (n.d.). *Hondsbossche en Pettemer Zeewering versterken kustlijn* (tech. rep.). https://nederland.boskalis.com/media/cbjjkwug/hondssbosche-en-pettermer-zeewering.pdf

Jacobs, J. (2019). Prediction of the closure of an artificial lagoon at the Dutch Coast: A case study on the lagoon at the Hondsbossche Dunes. https://repository.tudelft.nl/islandora/object/uuid:4d4a94c2-a5d6-4353-b14c-b6f0e9df4d1a?collection=education

Janssen, W. (2021, January). Wind in Nederland. https://www.weerplaza.nl/weerinhetnieuws/klimaat/wind-in-nederland/6820/

Jin, X., & Han, J. (2010). K-means clustering. In C. Sammut & G. I. Webb (Eds.), *Encyclopedia of machine learning* (pp. 563–564). Springer US. https://doi.org/10.1007/978-0-387-30164-8_425

KNMI. (n.d.). Naamgeving van stormen. https://www.knmi.nl/kennis-en-datacentrum/uitleg/naamgeving-van-stormen

Lague, D., Brodu, N., & Leroux, J. (2013). Accurate 3D comparison of complex topography with terrestrial laser scanner: Application to the Rangitikei canyon (N-Z). *ISPRS journal of photogrammetry and remote sensing*, *82*, 10–26. https://doi.org/10.1016/j.isprsjprs.2013.04.009

Lindenbergh, R., Van Der Kleij, S., Kuschnerus, M., Vos, S., & De Vries, S. (2019). CLUSTERING TIME SERIES OF REPEATED SCAN DATA OF SANDY BEACHES. *The international archives of the photogrammetry, remote sensing and spatial information sciences/International archives*

of the photogrammetry, remote sensing and spatial information sciences, *XLII-2/W13*, 1039–1046. https://doi.org/10.5194/isprs-archives-xlii-2-w13-1039-2019

Liu, F., & Deng, Y. (2021). Determine the number of unknown targets in open world based on elbow method. *IEEE Transactions on Fuzzy Systems*, *29*(5), 986–995. https://doi.org/10.1109/TFUZZ.2020.2966182

Longhitano, S. G. (2015). Short-Term Assessment of Retreating vs. Advancing Microtidal Beaches Based on the Backshore/Foreshore Length Ratio: Examples from the Basilicata Coasts (Southern Italy). *Open journal of marine science*, *05*(01), 123–145. https://doi.org/10.4236/ojms.2015.51011

Nichols, G. (2009, January). *Sedimentology and Stratigraphy*. http://ci.nii.ac.jp/ncid/BA91075174

NSO. (n.d.). Satellietdataportaal. https://www.spaceoffice.nl/nl/satellietdataportaal/

Pedregosa, F., Varoquaux, G., Gramfort, A., Michel, V., Thirion, B., Grisel, O., Blondel, M., Prettenhofer, P., Weiss, R., Dubourg, V., et al. (2011). Scikit-learn: Machine learning in python. *Journal of machine learning research*, *12*(Oct), 2825–2830.

py4dgeo Development Core Team. (2022). Py4dgeo: Library for change analysis in 4d point clouds. https://github.com/3dgeo-heidelberg/py4dgeo

QGIS Development Team. (2023). *Qgis geographic information system*. Open Source Geospatial Foundation. http://qgis.osgeo.org

Rokach, L., & Maimon, O. (2005). Clustering methods. In O. Maimon & L. Rokach (Eds.), *Data mining and knowledge discovery handbook* (pp. 321–352). Springer US. https://doi.org/10.1007/0-387-25465-X_15

Short, A., & Jackson, D. (2013, April). Beach morphodynamics. Elsevier. https://doi.org/10.1016/B978-0-12-374739-6.00275-X

Smith, N. P. (1986). The rise and fall of the Estuarine intertidal zone. *Estuaries*, *9*(2), 95. https://doi.org/10.2307/1351941

Van Wiechen, P., De Vries, S., Reniers, A., & Aarninkhof, S. (2023). Dune erosion during storm surges: A review of the observations, physics and modelling of the collision regime. *Coastal engineering*, *186*, 104383. https://doi.org/10.1016/j.coastaleng.2023.104383

Vos, S., Spaans, L., Reniers, A., Holman, R., Mccall, R., & De Vries, S. (2020). Cross-Shore Intertidal Bar Behavior along the Dutch Coast: Laser Measurements and Conceptual Model. *Journal of marine science and engineering*, *8*(11), 864. https://doi.org/10.3390/jmse8110864

Vos, S., van IJzendoorn, C., Lindenbergh, R., & De Wulf, A. (2024). Asynchronous dune development on a dutch urbanized beach due to buildings and other anthropogenic influences. *Geomorphology*.

Vosselman, G., & Maas, H. (Eds.). (2010). *Airborne and terrestrial laser scanning* [Once you have downloaded an eBook you need to open it once while you are connected to your network in order to activate the time stamp. After you have opened it once, you can then disconnect from the network and read as normal.]. CRC Press (Taylor & Francis).

Wang, Z., Shu, R., Xu, W., Pu, H., & Yao, B. (2008). *ANALYSIS AND RECOVERY OF SYSTEMATIC ERRORS IN AIRBORNE LASER SYSTEM* (tech. rep.). https://www.isprs.org/proceedings/xxxvii/congress/1_pdf/48.pdf

Winiwarter, L., Anders, K., & Höfle, B. (2021). M3c2-ep: Pushing the limits of 3d topographic point cloud change detection by error propagation. *ISPRS Journal of Photogrammetry and Remote Sensing*, *178*, 240–258. https://doi.org/https://doi.org/10.1016/j.isprsjprs.2021.06.011

A

Python code

In [ ]:
```
#importing the packages needed
import os
import numpy as np
import py4dgeo
from datetime import datetime
import pooch
import geopandas
import matplotlib.pyplot as plt
import matplotlib.dates as mdates
import matplotlib.lines as mlines
```

In [ ]:
```
#defining the colorbars
import matplotlib.colors
cvals  = [-4, -3, -2, -1, 0, 1, 2, 3, 4, 5, 6, 7, 8, 9]
blue = np.array([0/256, 0/256, 255/256,1])
purple = np.array([170/256, 0/256, 255/256,1])
indigo = np.array([170/256, 170/256, 255/256,1])
pink = np.array([255/256, 170/256, 255/256,1])
white = np.array([255/256, 255/256, 255/256,1])
green1 = np.array([170/256, 255/256, 127/256,1])
green2 = np.array([0/256, 255/256, 127/256,1])
green3 = np.array([0/256, 130/256, 0/256,1])
yellow = np.array([255/256, 255/256, 0/256,1])
orange1 = np.array([255/256, 217/256, 140/256,1])
orange2 = np.array([255/256, 136/256, 0/256,1])
red1 = np.array([255/256, 0/256, 0/256,1])
red2 = np.array([211/256, 0/256, 0/256,1])
red3 = np.array([148/256, 0/256, 0/256,1])
colors = [blue, purple, indigo, pink, white, green1, green2, green3, yellow, orange1
          orange2, red1, red2, red3]
colors_k = [blue, pink, green3, orange1, red2]

norm=plt.Normalize(min(cvals),max(cvals))
tuples = list(zip(map(norm,cvals), colors))
M3C2color = matplotlib.colors.LinearSegmentedColormap.from_list("", tuples)
```

In [ ]:
```
#importing the data
pc_dir = r'C:\Users\hoeks\Python\DataBEPcropped'
pc_list = os.listdir(pc_dir)
```

In [ ]:
```
#defining the dates of the data
times = ["16 February 2016", "27 January 2017", "13 February 2018",
         "24 February 2019","14 March 2020", "15 January 2021",
         "28 February 2022", "8 February 2023"]
timestamps = []
for i in range(len(times)):
    timestamp_str = times[i]
    timestamp = datetime.strptime(timestamp_str, "%d %B %Y")
    timestamps.append(timestamp)
```

In [ ]:
```
# Creating an analysis file
analysis = py4dgeo.SpatiotemporalAnalysis("analysis", force=True)

# Specify the reference epoch
reference_epoch_file = os.path.join(pc_dir, pc_list[0])

# Read the reference epoch and set the timestamp
```

```
reference_epoch = py4dgeo.read_from_las(reference_epoch_file)
reference_epoch.timestamp = timestamps[0]

# Set the reference epoch in the spatiotemporal analysis object
analysis.reference_epoch = reference_epoch
```

In [ ]:

```
#use the M3C2 vertical algorithm
class M3C2_Vertical(py4dgeo.M3C2):
    def directions(self):
        return np.array([0, 0, 1])  # vertical vector orientation


# Specify corepoints, here all points of the reference epoch
analysis.corepoints = reference_epoch.cloud[::]

# Specify M3C2 parameters for our custom algorithm class
analysis.m3c2 = M3C2_Vertical(
    cyl_radii=(1.0,), max_distance=10.0, registration_error=0.019)
```

In [ ]:

```
#calculate epoch objects
epochs = []
for e, pc_file in enumerate(pc_list[1:]):
    epoch_file = os.path.join(pc_dir, pc_file)
    epoch = py4dgeo.read_from_las(epoch_file)
    epoch.timestamp = timestamps[e+1]
    epochs.append(epoch)

# Add epoch objects to the spatiotemporal analysis object
analysis.add_epochs(*epochs)
```

In [ ]:

```
# Get the corepoints
corepoints = analysis.corepoints.cloud

# get change values of last epoch for all corepoints
distances = analysis.distances

# Get the list of timestamps from the reference epoch timestamp and timedeltas
timestamps = [t + analysis.reference_epoch.timestamp for t in analysis.timedeltas]
```

In [ ]:

```
# Allow interactive rotation in notebook

# Calculate the distances for each epoch
%matplotlib inline
datetimeoutput = "%d-%m-%Y"
def generate_distances(epoch, ax, n, point_index):
    distances_epoch = [d[epoch] for d in distances][::n]
    coord_sel_list = []
    for i in range(len(point_index)):
        coord_sel_i = analysis.corepoints.cloud[point_index[i]]
        coord_sel_list.append(coord_sel_i)
    coord_sel = np.matrix(coord_sel_list)
    d = ax.scatter(
        corepoints[:, 0][::n],
        corepoints[:, 1][::n],
        c=distances_epoch,
#         cmap="seismic_r",
        cmap = M3C2color,
        vmin=-4,
        vmax=9,
```

```
        s=1,
        zorder=1,
        )
    markers = ["P", "D", "s", "v", "o"]
    for i in range(len(point_index)):
        ax.scatter(
            coord_sel[i,0],
            coord_sel[i,1],
            facecolor="yellow",
            edgecolor="black",
            s=50,
            zorder=2,
            marker=markers[i],
            )

    ax.set_xlabel("X [m]")
    ax.tick_params(axis='x', labelrotation=60)
    ax.set_ylabel("Y [m]")
    ax.set_aspect("equal")
    ax.set_title(
    "Changes at %s"
    % (analysis.reference_epoch.timestamp +
       analysis.timedeltas[epoch]).strftime(datetimeoutput)
    )
    return d
```

In [ ]:

```
# Plot the M3C2 distances for each epoch
points = []
fig = plt.figure(figsize=(10, 10))

for i in range(7):
    ax = fig.add_subplot(2, 4, i+1)
    d = generate_distances(i,ax, 10, points)
fig.subplots_adjust(right=0.8)
cbar_ax = fig.add_axes([0.8, 0.07, 0.05, 0.4])
fig.colorbar(d, cax=cbar_ax, label = 'Distance [m]')
```

In [ ]:

```
# Import packages needed
from sklearn.cluster import KMeans
from sklearn import metrics
from scipy.spatial.distance import cdist

# Define the number of clusters
ks = [5,6, 7, 8, 9, 10]

# Create an array to store the labels
labels = np.full((distances.shape[0], len(ks)), np.nan)

# Perform clustering for each number of clusters
for kidx, k in enumerate(ks):
    print(f"Performing clustering with k={k}...")
    nan_indicator = np.logical_not(np.isnan(np.sum(distances, axis=1)))
    kmeans = KMeans(n_clusters=k, random_state=0).fit(distances[nan_indicator, :])
    labels[nan_indicator, kidx] = kmeans.labels_
```

In [ ]:

```
# Calculate the distortions for different amount of clusters
distortions = []
mapping1 = {}
K = range(1, 11)
nan_indicator = np.logical_not(np.isnan(np.sum(distances, axis=1)))
```

```
X = distances[nan_indicator, :]

for k in K:
    # Building and fitting the model
    kmeanModel = KMeans(n_clusters=k, random_state=0).fit(X)
    kmeanModel.fit(X)

    distortions.append(sum(np.min(cdist(X, kmeanModel.cluster_centers_,
                                        'euclidean'), axis=1)) / X.shape[0])
    inertias.append(kmeanModel.inertia_)

    mapping1[k] = sum(np.min(cdist(X, kmeanModel.cluster_centers_,
                                   'euclidean'), axis=1)) / X.shape[0]

# Plot the amount of clusters again the distortion
plt.plot(K, distortions, 'bx-')
```

In [ ]:

```
# Define colormaps
cvals_k5  = [0,1,2,3,4]
cvals_k6  = [0,1,2,3,4,5]
cvals_k7  = [0,1,2,3,4,5,6]
cvals_k8  = [0,1,2,3,4,5,6,7]
cvals_k9  = [0,1,2,3,4,5,6,7,8]

blue_k = np.array([31/256, 119/256, 180/256,1])
orange_k = np.array([255/256, 127/256, 14/256,1])
green_k = np.array([44/256, 160/256, 44/256,1])
red_k = np.array([214/256, 39/256, 40/256,1])
purple_k = np.array([148/256, 103/256, 189/256,1])
brown_k = np.array([140/256, 86/256, 75/256,1])
pink_k = np.array([227/256, 119/256, 194/256,1])
grey_k = np.array([127/256, 127/256, 127/256,1])
yellow_k = np.array([188/256, 189/256, 34/256,1])

colors_k5 = [blue_k, orange_k, green_k, red_k, purple_k]
colors_k6 = [blue_k, orange_k, green_k, red_k, purple_k, brown_k]
colors_k7 = [blue_k, orange_k, green_k, red_k, purple_k, brown_k,
             pink_k]
colors_k8 = [blue_k, orange_k, green_k, red_k, purple_k, brown_k,
             pink_k, grey_k]
colors_k9 = [blue_k, orange_k, green_k, red_k, purple_k, brown_k,
             pink_k, grey_k, yellow_k]

norm_k5=plt.Normalize(min(cvals_k5),max(cvals_k5))
tuples_k5 = list(zip(map(norm_k5,cvals_k5), colors_k5))
k5_cmap = matplotlib.colors.LinearSegmentedColormap.from_list("", tuples_k5)

norm_k6=plt.Normalize(min(cvals_k6),max(cvals_k6))
tuples_k6 = list(zip(map(norm_k6,cvals_k6), colors_k6))
k6_cmap = matplotlib.colors.LinearSegmentedColormap.from_list("", tuples_k6)

norm_k7=plt.Normalize(min(cvals_k7),max(cvals_k7))
tuples_k7 = list(zip(map(norm_k7,cvals_k7), colors_k7))
k7_cmap = matplotlib.colors.LinearSegmentedColormap.from_list("", tuples_k7)

norm_k8=plt.Normalize(min(cvals_k8),max(cvals_k8))
tuples_k8 = list(zip(map(norm_k8,cvals_k8), colors_k8))
k8_cmap = matplotlib.colors.LinearSegmentedColormap.from_list("", tuples_k8)

norm_k9=plt.Normalize(min(cvals_k9),max(cvals_k9))
tuples_k9 = list(zip(map(norm_k9,cvals_k9), colors_k9))
k9_cmap = matplotlib.colors.LinearSegmentedColormap.from_list("", tuples_k9)
```

In [ ]:

```
# Create the figure for clustering. This cell can be modified to plot
# the desired amount of clusters
n = 10
cmap_clustering = "tab20"
fig, axs = plt.subplots(1, 2, figsize=(12, 8))
(ax1, ax2) = axs


timestamps_strings = [ts.strftime(datetimeoutput) for ts in timestamps]

# Get the labels for the selected number of clusters
labels_k5 = labels[:,0]
labels_k6 = labels[:,1]
labels_k7 = labels[:,2]
labels_k8 = labels[:,3]
labels_k9 = labels[:,4]
labels_k10 = labels[:, 5]


# plot the map of clusters
sc = ax1.scatter(
    corepoints[:, 0][::n], corepoints[:, 1][::n], c=labels_k5[::n],
    cmap=k5_cmap, s=1)


# Plot the time series representing the clusters (median of each cluster)
for l in np.unique(labels_k5):
    ax2.plot(
        timestamps_strings,
        np.nanmedian(distances[labels_k5 == l, :], axis=0),
        label=f"cluster {l}",)
# Format the date labels
import matplotlib.dates as mdates


# Add plot elements
ax1.set_aspect("equal")
ax1.tick_params(axis='x', labelrotation=60)
ax1.set_title(f"# clusters = {ks[0]}")
ax2.set_xlabel("Date")
ax2.tick_params(axis='x', labelrotation=60)
ax2.set_ylabel("Distance [m]")
ax2.grid()
```

In [ ]:

```
# The volumes of the dunes over the different years, compared to the reference year
volume_dune1 = [3727.816, 6256.906, 14152.018, 24788.774,
                26701.544, -3540.893, 5342.305]
volume_dune2 = [-9204.054, -15066.179, -1400.413, -918.893,
                -10642.012, -25987.274, -10860.381]
volume_dune3 = [-1721.311, 4461.948, 10640.921, 23059.874,
                20205.139, 7010.563, 17329.184]
years = [2017, 2018, 2019, 2020, 2021, 2022, 2023]
# Plot the volumes over time
plt.plot(years, volume_dune1, label = 'Dune 1')
plt.plot(years, volume_dune2, label = 'Dune 2')
plt.plot(years, volume_dune3, label = 'Dune 3')
```